Theses and Dissertations

Spring 2016

State-dependent processing of reafference arising from self-generated movements in infant rats

Alexandre Tiriac
University of Iowa

Recommended Citation

STATE-DEPENDENT PROCESSING OF REAFFERENCE ARISING FROM

SELF-GENERATED MOVEMENTS IN INFANT RATS

by

Alexandre Tiriac

A thesis submitted in partial fulfillment
of the requirements for the Doctor of Philosophy
degree in Psychology in the
Graduate College of
The University of Iowa

May 2016

Thesis Supervisor: Professor Mark S. Blumberg

Graduate College
The University of Iowa
Iowa City, Iowa

CERTIFICATE OF APPROVAL

_____

PH.D. THESIS

_____

This is to certify that the Ph.D. thesis of

Alexandre Tiriac

has been approved by the Examining Committee for
the thesis requirement for the Doctor of Philosophy degree
in Psychology at the May 2016 graduation.

Thesis Committee: _____
                  Mark S Blumberg, Thesis Supervisor

                  _____
                  John H. Freeman

                  _____
                  Michelle W. Voss

                  _____
                  Ryan T. Lalumiere

                  _____
                  Daniel T. Tranel

For my grandparents
Three of them provided me with endless love
The fourth with a microscope

ACKNOWLEDGMENTS

ABSTRACT

Nervous systems distinguish between self- and other-generated movements by monitoring discrepancies between planned and performed actions. To do so, when motor systems transmit motor commands to muscles, they simultaneously transmit motor copies, or corollary discharges, to sensory areas. There, corollary discharge signals are compared to sensory feedback arising from movements (reafference), which can result in gating of expected feedback. Curiously, in infant rats, twitches—which are self-generated movements produced exclusively and abundantly during active sleep (AS)—differ from wake-movements in that they trigger robust neural activity. Accordingly, we hypothesized that the gating actions of corollary discharge that predict wake reafference are suspended during twitching. In this dissertation, we first demonstrate that twitches, but not wake movements, robustly activate sensorimotor cortex as they do other brain areas. Next, we demonstrate that wake movements can activate the sensorimotor cortex under conditions involving presumed discrepancies between corollary discharge and reafference signals. Lastly, we reveal a neural mechanism in the brainstem that inhibits reafference, but only during wakefulness; this inhibitory mechanism is suppressed during active sleep. All together, our findings provide the first demonstration of a state-dependent neural comparator of planned and performed actions, one that permits the transmission of sensory feedback from self-generated twitches to the developing nervous system.

PUBLIC ABSTRACT

It is easier for someone to tickle you than it is for you to tickle yourself. This is because tickling entails some level of surprise, and you can't surprise yourself. Therefore, your brain must have a mechanism that suppresses the sensations arising from self-tickling. This type of suppression lies at the heart of our ability to distinguish between the sensations that arise from our self-produced movements from those that arise from other-produced movements. Interestingly, whereas self-generated movements produced during wake are accompanied by this type of suppression, self-generated movements produced during active sleep (i.e., twitches) are not. Twitches are a predominant behavior of early development and are exhibited by all mammals. Yet, despite their predominance, the neural mechanisms that permit twitches to bypass sensory suppression are unknown. In this dissertation, we show that twitches, but not wake movements, robustly activate the brain. Moreover, we describe one neural mechanism that leads to the selective inhibition of wake-related activity, and show that this mechanism is located early in the pathway of sensory processing. Taken together, the results presented here demonstrate that twitches, despite being self-generated, are processed by the brain as if they are not. This novel aspect of twitching supports the view that twitching, by robustly activating the infant's sensorimotor system, contributes to its development.

TABLE OF CONTENTS

LIST OF FIGURES

LIST OF ABBREVIATIONS

REM: Rapid eye movement

MUA: Multi unit activity

LFP: Local field potential

M1:   Primary motor cortex

S1:   Primary somatosensory cortex

ECN: External cuneate nucleus

GABA: *gamma*-Aminobutyric acid

CHAPTER 1: INTRODUCTION

Infant rats, like all mammals, spend the majority of their time asleep, specifically in REM sleep (Jouvet-Mounier et al., 1970; Roffwarg et al., 1966). Although we typically think of sleep as a period of rest, REM sleep is dominated by motor activity (Seelke and Blumberg, 2008). This motor activity takes the form of myoclonic twitches, which are discrete movements of the limbs, tail, and even the facial muscles that control the lips, whiskers, and eyes (Petersson et al., 2003; Seelke et al., 2005; Tiriac et al., 2012). In rats and other mammals, twitches are already expressed embryonically (Milh et al., 2007; Robinson et al., 2008, 2000), are most frequent early in development (Gramsbergen et al., 1970; Jouvet-Mounier et al., 1970; Marcano-Reik et al., 2010), and persist throughout the lifespan (Gassel et al., 1964; Stefani et al., 2015).

In comparison to wake movements, twitches are typically of low amplitude and rarely occur in a conjugated manner; instead, they consist of rapid asynchronous flurries of movements throughout the body (Blumberg et al., 2013a). Despite being of lower amplitudes, twitches robustly trigger more reafference (sensory feedback arising from self-generated movements) throughout the neuraxis than wake movements (Sokoloff et al., 2015b; Tiriac et al., 2014). Recording from neurons of infant rats, we have demonstrated this disparity in reafference in the brainstem, cerebellum, thalamus, primary sensory and motor cortex, and hippocampus (Mohns and Blumberg, 2010; Sokoloff et al., 2015b; Tiriac et al., 2014, 2012); in the cortex, wake movements produced

virtually no reafference (Tiriac et al., 2014). The fact that twitches robustly activate the developing brain may be a clue as to their function, so understanding the neural mechanisms that permit them to activate the brain is necessary to that end. However, to understand why twitches trigger such pronounced reafference, it is helpful to understand why wake movements do not.

Fundamentals of corollary discharge

Animals can distinguish between sensations that arise from self-generated movements from those that arise from other-generated movements (Crapse and Sommer, 2008; Sommer and Wurtz, 2008). To do so, when producing a motor command, the nervous system simultaneously produces motor copies, or corollary discharges (Bell, 1989; Poulet and Hedwig, 2006; Sawtell, 2010; Sommer and Wurtz, 2002). Whereas a motor command is transmitted to muscles to produce a movement, a corollary discharge is transmitted to non-motor areas of the brain, typically sensory areas (Poulet and Hedwig, 2006; Sommer and Wurtz, 2002). This corollary discharge is then compared to the reafference of the movement, which can result in gating of expected reafference (Bell, 1989; Poulet and Hedwig, 2006; Sawtell, 2010).

The concept of corollary discharge has been demonstrated in many organisms. Worms, for example, display a stereotypical withdrawal reflex when their head is unexpectedly stimulated. As these animals move, their bodies receive constant sensory stimulations from the outside world (e.g., from water or dirt touching the body). Yet, despite these sensations, worms are able to

continue moving forward without constantly triggering the withdrawal reflex. This is because when the worm moves, the motorneurons that are responsible for the animal's motility transmit corollary discharges that inhibit incoming sensory feedback (Crapse and Sommer, 2008).

As another example, crickets communicate by chirping, a loud sound that is produced by the vibration of their forewings (Hedwig, 2006). As chirps are produced, the cricket's motor neurons transmit corollary discharge signals that suppress all incoming auditory feedback (Poulet and Hedwig, 2006), thereby preventing the desensitization of auditory receptors. Both worms and crickets exhibit what is referred to as lower-order corollary discharge because the suppression of sensory feedback is an all-or-none process (Crapse and Sommer, 2008). Although this type of inhibition is sufficient for preventing reflexes or desensitization of receptors, it blocks all incoming sensory stimuli, both arising from self-generated action and externally induced stimuli. As such, lower-order corollary discharge mechanisms do not permit the nervous system to discriminate between expected and unexpected stimuli in the midst of ongoing behavior.

Unlike lower-order corollary discharge mechanisms, higher-order mechanisms permit the behaving animal to monitor the external environment for unexpected events. For example, the mormyrid fish scans its external environment by generating an electric organ discharge (EOD; Caputi, 2004). When these EODs are generated, an electric organ corollary discharge (EOCD) of the pulse is transmitted to parts of the brain that process reafference arising

from electroreceptors. When no perturbations in the electrical environment occur, the EOCD signal accurately predicts the incoming reafference and gates it completely. When the EOCD does not match the reafference, as would be the case with unexpected events, the portion of the reafference that is unexpected is passed through the gating mechanism (Bell, 1989). Therefore, in this particular case of active sensing, corollary discharge mechanisms selectively gate expected reafference and allow unexpected reafference to pass through.

In primates, motion of the head is monitored carefully via the actions of corollary discharge. During voluntary self-motion, cells of the deep cerebellar nuclei that receive vestibular afferents are not responsive to the movement. However, the addition of an unexpected load to the head during self-motion creates a mismatch between the corollary discharge and reafference signals. In this scenario, the neurons of the deep cerebellar nuclei exhibit an increased firing rate in response to the movement. Interestingly, if the load is maintained, the firing rate of deep cerebellar neurons returns to baseline over time, suggesting that animals can rapidly update its predictions of the sensory consequences of self-generated movements (Brooks et al., 2015).

Are twitches unexpected self-generated movements?

In the context of infant rats, we hypothesized that wake movements are processed by the nervous system as if they are expected. Mechanistically, this would mean that corollary discharge signals are produced during wake movements that ultimately inhibit expected reafference. In contrast, the robust

4

reafference observed during active sleep would suggest that twitches are processed by the nervous system as if they are unexpected. Mechanistically, this would mean that corollary discharge signals are either absent or inhibited during twitching, resulting in more neural activity.

To test our hypotheses, we performed neural recordings in unanaesthetized head-fixed infant rats that were cycling between sleep and wake (Blumberg et al., 2015). A critical piece of this setup is that the pup's limbs dangle freely, which entails the following: 1) Without experimental manipulations, self-generated movements of dangling limbs do not trigger unexpected reafference; and 2) easy access to the limbs allows the experimenter to manipulate the expectancy of self-generated movements.

In Chapter 2, we first recorded from the hindlimb region of sensorimotor cortex and established that it, like the cerebellum (Sokoloff et al., 2015b), thalamus (Khazipov et al., 2004; Tiriac et al., 2012), and hippocampus (Mohns and Blumberg, 2010), exhibits more activity during sleep than wake (Tiriac et al., 2014). Next, we tested whether the lack of wake-related activity was due a global, non-specific inhibition of sensory feedback during wake. We provide evidence against this hypothesis by demonstrating that stimulation of the hindlimb triggers just as much sensory feedback during sleep than during wake. Lastly, we pharmacologically and behaviorally induced self-generated movements during wake that were designed to minimally recruit corollary discharge pathways. We found that these induced movements, unlike spontaneous wake movements, trigger robust sensory activity in the

5

sensorimotor cortex. In summary, these findings strongly suggest that the actions of corollary discharge that normally gate reafference arising from wake movements are either absent or inhibited during twitching.

In search of a state-dependent neural comparator

If the nervous system indeed selectively gates wake-related reafference, then there must be a neural structure somewhere in the sensory neuraxis that acts as a state-dependent comparator of corollary discharge and reafference signals. To be a comparator, a brain nucleus must integrate sensory and motor signals. For example, in the mormyrid fish described above, the electrosensory lateral line lobe (ELL) receives both primary afferents from electroreceptors and inputs conveying the EOCD (Bell, 1989).

In rats, proprioceptive inputs arising from muscle spindles in the forelimbs terminate in the external cuneate nucleus (ECN), which is located in the caudal medulla (Campbell et al., 1974). These primary afferents are glutamatergic. In addition, the ECN receives GABAergic and glycinergic inputs, thereby providing a possible mechanism of sensory modulation (Galindo et al., 1967; Heino and Westman, 1991; Sato et al., 1991). Moreover, the ECN receives direct input from at least two separate motor areas: Propriospinal premotor neurons (PNs; Pivetta et al., 2014) and the red nucleus (Edwards, 1972; Holstege and Tan, 1988; Martin et al., 1974). Although the function of these pathways to the ECN is not known, a corollary discharge pathway from PNs to another medullary structure, the lateral reticular nucleus, has been described (Alstermark et al., 2007; Azim et

al., 2014; Pivetta et al., 2014). Taken together, the anatomy of the ECN suggests a potential role as a comparator.

We therefore aimed to record from the ECN to investigate its potential role as a neural comparator of planned and performed actions. In Chapter 3, we demonstrate that the ECN, like the sensorimotor cortex, displays more activity during twitching than during wake movements. We show that wake-related reafference is unmasked by blockade of GABA and glycine receptors in the ECN. Critically, disinhibition of the ECN has no effect on twitch-related reafference. These results demonstrate that the ECN does indeed act as a neural comparator, but does so only during wake.

In summary, the studies described in this dissertation demonstrate the following: 1) Twitches, but not wake movements, robustly activate the sensory neuraxis; 2) the lack of sensory activity during wake is not due a global inhibition of sensory feedback; 3) the ECN gates reafference, but only during wake; and (4) during active sleep, twitch-related reafference is not gated by the ECN. All together, our findings demonstrate that twitches are unique in that they are allowed to consistently and robustly activate the sensory neuraxis.

CHAPTER 2: SELF GENERATED MOVEMENTS WITH "UNEXPECTED" SENSORY CONSEQUENCES

Introduction

The nervous systems of diverse species, including worms and humans, possess mechanisms for distinguishing between sensations arising from self-generated (i.e., expected) movements from those arising from other-generated (i.e., unexpected) movements (Crapse and Sommer, 2008; Cullen, 2004; Poulet and Hedwig, 2007). To make this critical distinction, animals generate copies, or corollary discharges, of motor commands (Holst and Mittelstaedt, 1950; Sperry, 1950). Corollary discharge facilitates the selective gating of reafferent signals arising from self-generated movements, thereby enhancing detection of novel stimuli (Bell, 2001; Brooks and Cullen, 2013; Kennedy et al., 2014; Poulet and Hedwig, 2006; Sommer and Wurtz, 2002). However, for a developing nervous system, such sensory gating would be counterproductive if it impedes transmission of the very activity upon which activity-dependent mechanisms depend (Kirkby et al., 2013). In infant rats during active (or REM) sleep—a behavioral state that predominates in early infancy (Gramsbergen et al., 1970; Jouvet-Mounier et al., 1970; Roffwarg et al., 1966; Scriba et al., 2013; Thurber et al., 2008)—neural circuits within the brainstem (Karlsson et al., 2005; Kreider and Blumberg, 2000) trigger hundreds of thousands of myoclonic twitches each day (Blumberg et al., 2013b). The hypothesized role for these self-generated movements in the activity-dependent development of the sensorimotor system is

supported by the observation that reafference from twitching limbs reliably and substantially triggers brain activity (Khazipov et al., 2004; Mohns and Blumberg, 2010; Sokoloff et al., 2015b; Tiriac et al., 2012). In contrast, under identical testing conditions, even the most vigorous wake movements reliably fail to trigger reafferent brain activity (Mohns and Blumberg, 2010; Sokoloff et al., 2015b; Tiriac et al., 2012). To account for this paradox, it was hypothesized that twitches, uniquely among self-generated movements, lack corollary discharge (Sokoloff et al., 2015b). Here, we test this hypothesis in newborn rats by manipulating the degree to which self-generated movements are expected and, therefore, their presumed recruitment of corollary discharge. We show that twitches, although self-generated, are processed as if they are unexpected.

Experimental procedures

All experiments were carried out in accordance with the National Institutes of Health Guide for the Care and Use of Laboratory Animals (NIH Publication No. 80-23) and were approved by the Institutional Animal Care and Use Committee of the University of Iowa.

Subjects

A total of 44 Sprague-Dawley Norway rats (Rattus norvegicus) were used between the ages of 4 and 12 days of age. Males and females were used and littermates were always assigned to different experimental groups. Litters were culled to 8 pups within 3 days of birth. Mothers and their litters were housed in

standard laboratory cages (48 x 20 x 26 cm). Food and water were available ad libitum. All animals were maintained on a 12:12 light-dark schedule with lights on at 0700 h.

Surgery

Head-fix preparation. For all studies, pups were prepared for testing using methods similar to those described previously (Karlsson et al., 2005; Mohns and Blumberg, 2010; Tiriac et al., 2012). Under isoflurane anesthesia, bipolar electrodes (50 µm diameter; California Fine Wire) were implanted into the extensor digitorum longus muscle of the hindlimb and the nuchal muscle. The skin overlying the skull was removed and a custom-built head-fix apparatus was attached to the skull with cyanoacrylate adhesive. A small hole was drilled over the hindlimb region of primary motor cortex (M1; coordinates in relation to bregma: AP: -1.5 mm, L: 0.5 mm). In preliminary experiments, it was determined that electrical stimulation at this location of M1 produces movements of the contralateral hindlimb. After surgery, the pup was transferred to a humidified incubator maintained at thermoneutrality ($35^{o}C$) to recover for at least 1 hour, after which it was transferred to a stereotaxic apparatus. The pup's torso was supported on a narrow platform such that the limbs dangled freely on both sides. The pup acclimated for at least 1 additional hour before recordings began, by which time it was cycling between clear periods of sleep and wake.

Electrophysiological Procedures

The EMG electrodes were connected to a differential amplifier (A-M Systems, Carlsborg, WA; amplification: 10,000x; filter setting: 300-5000 Hz). To record from motor cortex, 16-channel silicon depth electrodes (100 µm vertical separation; NeuroNexus, Ann Arbor, MI), with impedances ranging from 1-4 MΩ, were connected to a headstage and data acquisition system (Tucker-Davis Technologies, Alachua, FL) that amplified (10,000x) and filtered the signals. Of the 16 channels, every other one was filtered for local field potentials (LFPs) or multi-unit activity (MUA). To record LFPs, the signals were filtered using a 1-40 Hz band-pass. For MUAs, the signals were filtered using a 500-5000 Hz band-pass. A 60 Hz notch filter was also used. Neurophysiological and EMG signals were sampled at 12.5 kHz and 1 kHz, respectively, using a digital interface and Spike2 software (Cambridge Electronic Design, Cambridge, UK).

Prior to insertion of the silicon probe, the electrode surface was coated with fluorescent DiI (Life Technologies, Carlsbad, CA) for subsequent histological verification of electrode placement. A Ag/AgCl ground electrode (Medwire, Mt. Vernon, NY, 0.25 mm diameter) was placed into the visual cortex ipsilateral to the silicon probe. Brain temperature was monitored using a fine-wire thermocouple (Omega Engineering, Stamford, CT) placed in the visual cortex contralateral to the ground wire. For all experiments, brain temperature was maintained at 36-37˚C.

The electrode was positioned above motor cortex and was lowered to a depth of 0.5-1.0 mm. Electrode position was set once it was possible to reliably

evoke neural activity by gentle stimulation of the contralateral hindlimb. Using procedures similar to those described previously (Karlsson et al., 2005; Mohns and Blumberg, 2010; Tiriac et al., 2012), data acquisition began after LFP signals were identified and had stabilized for at least 10 min; we also sought to record MUA activity but this was not always possible, especially at the younger ages. Recording sessions comprised continuous collection of neurophysiological and EMG data for at least 30 min. During acquisition, an experimenter monitored the subject's behavior and digitally marked the occurrence of sleep-related twitching and wake movements in synchrony with the physiological data. As described elsewhere (Karlsson et al., 2005), myoclonic twitches are phasic, rapid, and independent movements of the limbs and tail against a background of muscle atonia; in contrast, wake movements, which are high-amplitude, coordinated movements occurring against a background of high muscle tone, include locomotion, stretching, and yawning. Finally, the experimenter was always blind to the physiological data when scoring behavior.

Experimental Manipulations

Hindlimb stimulation. The hindlimb contralateral to the recording site was stimulated using a fine paintbrush every 5-10 s for 10 min. The brush was applied to the base of the paw and the limb was flexed at the knee. The stimulations were performed similarly during sleep and wake. The ipsilateral hindlimb as well as both forelimbs were also stimulated to confirm the specificity of the M1 response.

Pharmacological activation of hindlimb movements with quipazine. In 12 head-fixed P8-10 rats, M1 activity was recorded during a 15-min baseline period ("pre"). At the end of this baseline period, pups received a 0.1 ml intraperitoneal injection of the serotonin agonist, quipazine (Sigma-Aldrich, St. Louis, MO; dose: 3.0 mg/kg), or physiological saline (N=6 in each group). Five min after injection, M1 activity was recorded for an additional 15 min ("post").

Stimulation-induced triggering of hindlimb activity. In six head-fixed P8-10 rats, M1 activity was recorded in response to two types of stimulation, each designed to produce hindlimb movements via a different mechanism. First, to produce hindlimb activity via generalized arousal, a cold spatula was applied to the pup's snout (Todd et al., 2010). Second, to produce hindlimb activity via a local spinal circuit, the experimenter flicked the pup's tail. Both types of stimulation were presented during wakefulness, 2 s after wake movements had subsided. When a stimulation was applied, the experimenter marked the event on the computer keyboard. The two types of stimulation were presented 15 times each in an intermixed, randomized order, with an inter-stimulation interval of at least one min. A stimulation was deemed successful if it elicited a hindlimb movement; on those rare occasions when a stimulation was not successful, that trial was not counted toward the total of 15 and was not included in the data analysis.

Mid-thoracic spinal transection. In two P8-10 rats under isoflurane anesthesia, the skin above the mid-thoracic spinal cord was cut. The brown adipose tissue

was gently peeled back to expose the vertebral column. At T8-T9, a blunt forceps was used to expose the spinal cord, which was then completely cut using fine scissors. The brown adipose tissue was replaced and the incision was closed using Vetbond (3M, Maplewood, MN). Each pup was then head-fixed and prepared for M1 recording as already described. For these pups, the methods used for testing were identical to those described above for general arousal and tail flick. After this protocol was complete, the pups were then injected with quipazine, again using the same methods as those described above.

Histology

At the end of each experiment, the pup was overdosed with sodium pentobarbital (1.5 mg/g) and perfused transcardially with phosphate buffered saline followed by 4% paraformaldehyde. Brains were sectioned at 50 µm using a freezing microtome (Leica Microsystems, Buffalo Grove, IL). Recording sites were verified by visualizing the DiI tract at 5-10X magnification using a fluorescent Leica microscope (Leica Microsystems, Buffalo Grove, IL). Tissue slices were then stained using cresyl violet and the location of the recording site was identified. For the two additional animals with spinal transections, the spinal cord was visualized using a surgical microscope and the completeness of the transection was confirmed.

Data Analysis

Spike sorting and spindle burst analysis. As described previously (Sokoloff et al., 2015b), spike sorting was performed in Spike2 (Cambridge Electronic Design, Cambridge, UK). Spindle bursts were defined as comprising at least 3 oscillations, a dominant frequency of 10-15 Hz, and a duration of at least 100 ms (Khazipov et al., 2004). To aid in the identification of spindle bursts, the LFP channels were filtered using a 50 Hz low-pass filter. Next, the channel was converted using root mean square (RMS) with a time constant of 0.1 s. Five high-amplitude spindle bursts were averaged and the baseline value of the RMS channel was calculated. The midpoint between those two values was used as a threshold for identification of spindle bursts. A second pass through the data was performed to manually remove any spindle bursts that did not match the requisite criteria. Throughout this process, artifacts in the LFP and MUA signals were identified and manually removed.

Identification of behavioral state. Sleep and wake periods were defined using methods described previously (Karlsson et al., 2005; Mohns and Blumberg, 2010; Tiriac et al., 2012). Briefly, the nuchal EMG signal was dichotomized into periods of high tone (indicative of wake) and atonia (indicative of sleep). Moreover, active sleep was characterized by the occurrence of myoclonic twitches against a background of muscle atonia (Seelke and Blumberg, 2008). Spikes of EMG activity with amplitudes greater than 3x baseline were considered twitches.

Analysis of state-dependency. The mean rates of spindle burst production and unit activity were determined for each bout of wake and active sleep for each pup (there were at least 20 bouts of wake and active sleep for each pup). First, for each pup individually, successive bouts of wake and active sleep were treated as pairs and the Wilcoxon matched-pairs signed-ranks test (SPSS, IBM, Armonk, NY) was used to test for differences in rates of spindle burst production and unit activity between the two states. Although these data are not presented here, these rates were always significantly higher during active sleep than during wake. Second, the mean rates of spindle burst production and unit activity during wake and active sleep were calculated for each pup and compared within each age group using paired t tests. For all tests, alpha was set at 0.05.

Event correlations and waveform averages. The relationship between twitches and M1 activity was assessed as follows: First, the data for all pups within each age or experimental group were concatenated into one file. From this file, using twitches as triggers, event correlations (composed of 40 25-ms bins) of unit activity and waveform averages of spindle activity were constructed using a 1-s window. We tested statistical significance for both event correlations and waveform averages by jittering twitch events 1000 times within a 500-ms window using PatternJitter (Amarasingham et al., 2012). Then, using a custom-written Matlab program (MathWorks, Natick, MA), a 99% (P < .01) or 99.9% (P < .001) probability threshold was determined for each of the bins on either side of a twitch.

16

Differences in LFP power between experimental conditions were tested by first determining, for each pup, maximum power within the 1-s window. Similarly, differences in unit activity were tested by first determining, for each unit, the maximum firing rate over all 40 bins within the 1-s window. Paired t tests were then used to assess statistical significance.

Stimulus-triggered event correlations and waveform averages. The 10-min recordings from the hindlimb stimulation trials were divided into periods of sleep and wake. Event correlations (for unit activity; composed of 80 25-ms bins) and waveform averages (for LFPs) were constructed using a 2-s window and hindlimb stimulation as the trigger. We tested statistical significance using the jittering method described above.

For the experiment comprising application of a cold spatula to the snout (i.e., general arousal) and tail flick (i.e., spinally generated reflex), the first hindlimb movement (as determined using EMG) within 3 seconds of the presentation of a stimulus was marked as an event. These events were next collected into two groups (i.e., general arousal and spinal reflex). Finally, event correlations (for unit activity) and waveform averages (for LFPs) were constructed and statistical significance was determined using the jittering method.

Pharmacological activation of hindlimb movements with quipazine. For each pup in the 15 min before and after quipazine or saline administration, periods of active

wakefulness were identified when muscle tone was high and continuous limb movements were observed. The total amount of time that the contralateral hindlimb was moving, the number of spindle bursts, and the number of action potentials were quantified. To evaluate the influence of quipazine administration on hindlimb movements, spindle bursts, and unit activity, we performed a 2 x 2 repeated-measures factorial ANOVA (SPSS, IBM, Armonk, NY). The pharmacological condition (quipazine or saline) served as the between-subjects factor and time (pre- or post-injection) as the repeated-measures factor. For these tests, alpha was set at 0.05.

Results

Unanesthetized 8-10-day-old rats (n = 11) cycled between sleep and wakefulness while head-fixed in a stereotaxic apparatus with the limbs dangling freely (Figure 1A). We used 16-channel silicon electrodes to record extracellular neural activity from the hindlimb region of primary motor cortex (M1). We chose to record from M1 because, contrary to its designation as a motor structure, it also processes sensory (including proprioceptive) information (Hatsopoulos and Suminski, 2011), beginning early in development (An, 2013); this feature of M1 makes it well suited for investigations of sensorimotor integration. In pilot experiments, we established the coordinates of the hindlimb region of M1 using electrical stimulation to specifically elicit contralateral hindlimb movements. For every pup, we confirmed electrode location by manually stimulating the

contralateral hindlimb and verifying a sensory response in M1. Histology confirmed that electrodes were located in agranular cortex (Figure 1B, left).

The linear arrangement of the electrode sites (100 μm between sites) allowed for simultaneous recording from multiple cortical layers. Every other electrode site was filtered to identify spindle bursts in the local field potential (LFP; Figure 1B, right, blue traces) or multiunit activity (MUA; Figure 1B, right, black traces). All recorded units were located in the deep layers of M1. Spindle bursts were defined as described previously (Khazipov et al., 2004; Figure 1B, blue highlight).

Hindlimb Reafference Triggers M1 Activity in a State-Dependent Manner

As shown in Figure 1C for a representative recording, both LFP and MUA activity in M1 occurred predominantly during periods of active sleep, as indicated by muscle atonia and the presence of myoclonic twitches. In contrast, this activity was suppressed during periods of wake, as indicated by the high muscle tone (gray boxes). Across all pups, there was a significant increase in mean rates of spindle bursts (t_{10} = 9.2, p < 0.01) and mean unit firing rates (t_{16} = 3.2, p < 0.01, n = 17 units) during sleep (Fig 1D). Moreover, LFP power and unit activity increased after twitches within 100-125 ms (p < 0.001; Figure 1E). These results were replicated in 4- and 12-day-old rats, demonstrating the stability of the effect across early development (Figure 2).

Hindlimb Exafference Reliably Triggers M1 Activity Regardless of State

By design, because pups' limbs dangled freely in the apparatus, there was no opportunity for unexpected reafference. Consequently, the lack of activity after wake-related movements is consistent with the idea that corollary discharge gates or cancels the expected reafference from self-generated movements (Crapse and Sommer, 2008; Cullen, 2004) (Figure 3A). In contrast, manual stimulation of the hindlimb cannot be accompanied by corollary discharge and is therefore unexpected. Accordingly, we predicted that exafference would trigger M1 activity regardless of behavioral state, including the overall level of muscle tone (Figure 3B). We tested this hypothesis by manually flexing the hindlimb contralateral to M1 using a fine paintbrush. These stimulations were performed every 3-5 seconds for 10 min during periods of sleep and wake. Figure 4A depicts representative stimulations (arrows) performed during each state and the neural responses that follow these stimulations. As predicted, across all pups tested (n = 11), we observed significant increases in both LFP power and unit activity in response to stimulations regardless of behavioral state (p < 0.001; Figure 4B). Importantly, because exafference was transmitted to M1 during periods of high muscle tone (see Figure 4A, right), muscle tone alone cannot account for the wake-related gating of reafference. Finally, there was no significant difference in maximum LFP power between sleep and wake ($t_{10} = 1.3$); in contrast, there was a small (<10%) but significant difference in maximum unit firing rate ($t_{16} = 4.1$, p < 0.005). In any event, it is clear that exafference, in contrast to reafference, is reliably transmitted to M1 during both sleep and wake.

"Unexpected" Self-Generated Movements Trigger M1 Activity

Having demonstrated that other-produced movements trigger exafferent activation of M1, we next sought to assess the conditions under which self-produced movements trigger reafferent activation of M1. First, in 8-10-day-old rats, we injected a nonselective 5-HT agonist, quipazine (3.0 mg/kg ip), which is known to activate lumbar motorneurons (Brumley and Robinson, 2005). In this way, we aimed to activate hindlimb movements while minimizing the likelihood of engaging corollary discharge generators involved in modulating M1 activity (Figure 3C). We recorded M1 activity before and after quipazine or saline injection (Figure 5A). Hindlimb movements, rate of spindle burst activity, and unit firing rate all increased significantly after quipazine administration. Specifically, for hindlimb movements, we found significant main effects of group ($F_{1,10} = 59.7$, $p < 0.001$) and time ($F_{1,10} = 184.8$, $p < 0.001$), and a significant group x time interaction ($F_{1,10} = 271.8$, $p < 0.001$; Figure 5B). For spindle bursts, we found significant main effects of group ($F_{1,10} = 24.5$, $p < 0.01$) and time ($F_{1,10} = 14.0$, $p < 0.01$), and a significant group x time interaction ($F_{1,10} = 29.2$, $P < 0.001$; Figure 5C). Finally, only 4 pups in each group yielded clear M1 units; nonetheless, for unit activity, we found a significant main effect of group ($F_{1,6} = 7.3$ $p < 0.05$), a non-significant main effect of time ($F_{1,6} = 4.8$, $p = 0.07$), and a marginally significant group x time interaction ($F_{1,6} = 5.9$, $p = 0.05$; Figure 5C). These results suggest that reafference from unexpected self-generated movements are conveyed to M1. They also suggest that spinal motoneurons and associated local

circuitry are downstream from the generators of corollary discharge that suppress reafference associated with wake-related limb movements.

Because quipazine was injected systemically, we wanted to ensure that the M1 activity we observed was due to effects on spinal motoneurons. Therefore, in two additional P8-10 rats, we performed mid-thoracic spinal transections, thereby severing communication between the lumbar spinal cord and brain (Figure 6A). Injection of quipazine in the transected pups evoked hindlimb movements, similar to those in the non-transected pups (Figure 6B, top row). However, unlike the non-transected pups, spindle burst activity did not increase after quipazine injection in the transected pups, thus suggesting that the earlier results arose from quipazine's direct effects on spinal circuits.

We next devised a method to contrast the effects on M1 activity of expected and unexpected reafference arising from self-generated movements. To produce unexpected reafference, we flicked the tail, thereby engaging local spinal circuits to cause reflexive hindlimb movements (Figure 7A, red trace). In the same pups, to produce expected reafference, we applied a cold stimulus to the snout, thereby evoking generalized arousal and voluntary hindlimb movements (Todd et al., 2010) (Figure 7A, blue trace). Figure 7B presents representative data for the two manipulations. Both tail flick and application of the arousing stimulus (black arrows) elicited self-produced hindlimb movements (green arrows). As predicted, hindlimb movements elicited by tail flick, but not those elicited by the arousing stimulus, triggered significant increases in LFP power and unit activity in M1 ($p < 0.01$; Figure 7C). Moreover, maximum values

for both LFP and unit activity were significantly greater in response to tail flick than to the arousing stimulus (LFP: $t_5 = 4.1$, $p < 0.01$; MUA: $t_5 = 65.3$, $p < 0.001$).

To ensure that tail flicks did indeed activate local spinal circuitry, we performed tail flicks and arousing stimulations in the same two pups with mid-thoracic spinal transections described above. In the transected pups, flicks of the tail triggered hindlimb reflexes without affecting M1 LFP power (Figure 6B, bottom row). In contrast, arousing stimulation still continued to arouse the transected pups (e.g., forelimb movements); however, as expected, neither hindlimb movements nor increases in M1 LFP power was observed (data not shown).

Discussion

The absence of M1 activity during self-generated wake-related movements, as observed here, is consistent with prior reports describing differential sleep- and wake-related neural activity in the thalamus, somatosensory cortex, hippocampus, and cerebellum (Mohns and Blumberg, 2010, 2008; Sokoloff et al., 2015b; Tiriac et al., 2012). This absence of M1 activity, coupled with the reliable activation of M1 from exafferent stimulation, suggests the operation of corollary discharge in association with wake-related movements (Figures 3A and 3B). Similarly, in primates, passive head movements drive neural activity in the vestibular nuclei whereas active head movements do not, suggesting the selective cancelling of reafference by corollary discharge signals (Roy and Cullen, 2004). To further test the hypothesis that corollary discharge is

functioning early in development, we manipulated the expectancy or predictability of the reafference from self-generated movements (Figure 3C). Only unpredictable reafference reliably drove M1 activity, similar to what we observed with twitches (Figure 3D). To our knowledge, this is the first demonstration of a self-generated movement that is processed as if it were an other-generated movement and, therefore, unexpected.

Recent evidence suggests that corollary discharge suppresses proprioceptive reafference from the hindlimbs in Clarke's column neurons located in the thoracic and lumbar spinal cord (Hantman and Jessell, 2010). At this time, however, little is known about the neural sources of twitches and waking movements, especially early in development, thus preventing identification of the neural sources of corollary discharge or the neural sites where it modulates reafference. Therefore, an important next step is to determine whether the brainstem mechanisms that trigger twitches do not simultaneously generate corollary discharge or, alternatively, whether corollary discharge is generated but its effects are somehow inhibited. Regardless of the exact mechanism, the downstream effects on M1 activity would be the same.

Under normal waking conditions, corollary discharge makes it possible to account for expected reafferent signals triggered by one's own movements so that one is able to detect and respond appropriately to unexpected stimuli in the environment. Such accounting entails the gating or cancelling of reafference from self-generated movements. However, for the development and maintenance of precise, integrated, and hierarchically organized sensorimotor maps, infants

require high-fidelity information about the functional properties of limbs, muscles, and joints (Blumberg et al., 2013a; Marques et al., 2013). Our results suggest that such fidelity is achieved by suspending corollary discharge mechanisms during twitching, providing the infant with conditions ideally suited for activity-dependent development of the spinal cord (Petersson et al., 2003), cerebellum (Sokoloff et al., 2015b), and forebrain (Khazipov et al., 2004; McVea et al., 2012; Mohns and Blumberg, 2010; Tiriac et al., 2012). The information provided by twitching limbs may also enable the construction of internal models and predictive codes thought to be essential for flexible and efficient sensorimotor control and normal cognitive function (Frith et al., 2000; Shipp et al., 2013; Wolpert et al., 1998).
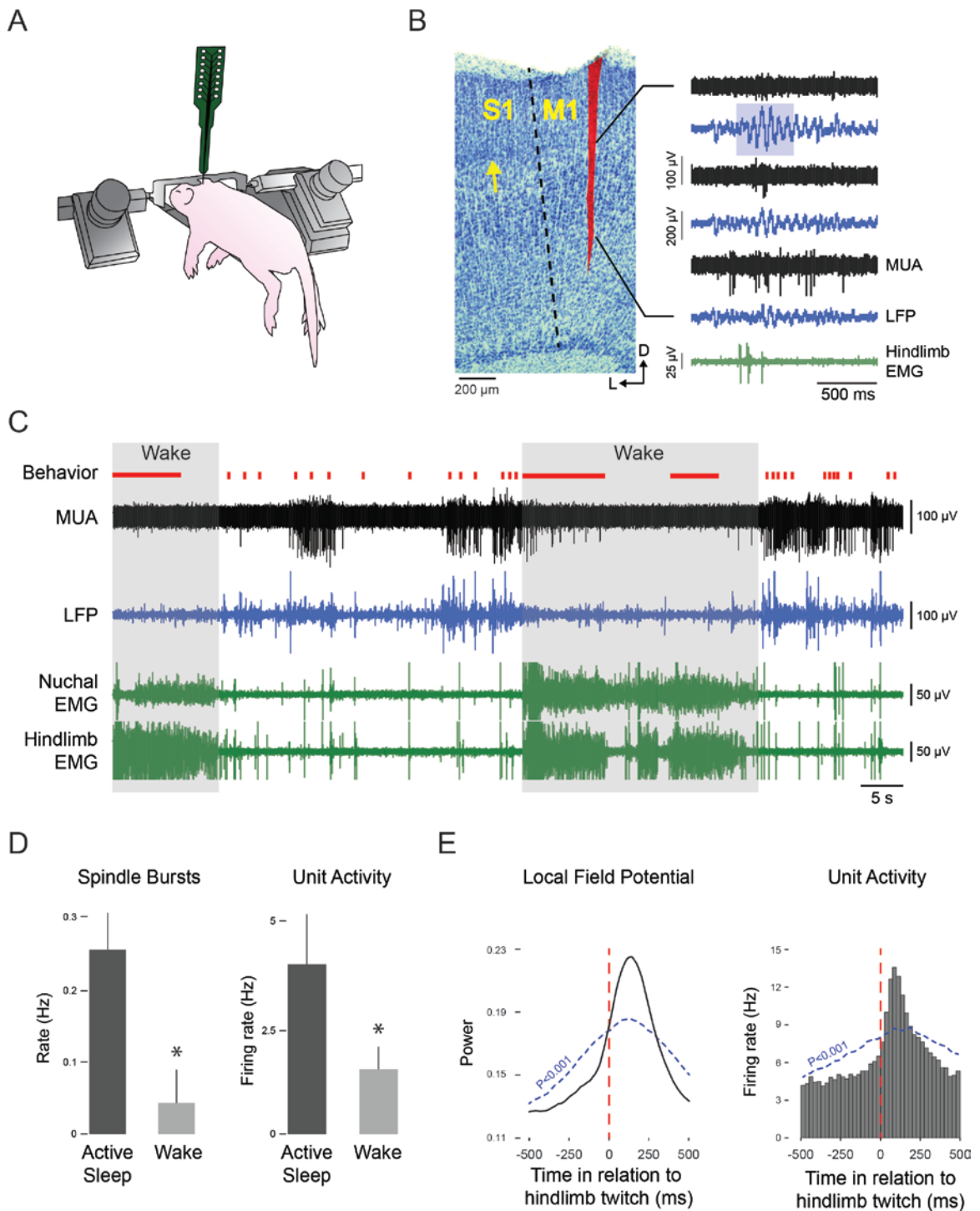
Figure 1. **Hindlimb twitches, but not wake-related hindlimb movements, trigger M1 activity**. (A) For these recordings, P8-10 rats were head-fixed in a stereotaxic apparatus and maintained at thermoneutrality. The torso was

supported by a platform and the limbs dangled freely. (B) Left: Coronal brain section, stained with cresyl violet, depicts the electrode track for a P10 subject. M1 is medial to primary somatosensory cortex (S1) and is agranular; the granular cell layer in S1 is denoted by the arrow. Right: Recordings from six sequential electrode sites with 100 µm separation. Signals are alternately filtered for multiunit activity (MUA; blue traces) and local field potentials (LFP; black traces). The spindle burst (blue highlighting) co-occurs with a burst of action potentials after a hindlimb twitch (green trace). (C) Representative data depicting sleep and wake behavior, MUA, LFP, and nuchal and hindlimb EMG during spontaneous sleep-wake cycling. Wake periods, characterized by high muscle tone, are highlighted in gray. Red tick marks denote hindlimb twitches and red horizontal lines denote hindlimb wake movements. (D) Mean (+ SEM) rate of spindle burst (n = 11) and unit activity (n = 17) during active sleep and wake periods. * significant difference from other group, $p < 0.05$. (E) Waveform average and event correlation for LFP power and unit activity, respectively, in relation to hindlimb twitches for data pooled across all subjects (4047 and 6358 twitches, respectively). Thresholds for statistical significance are indicated by the dotted blue lines.
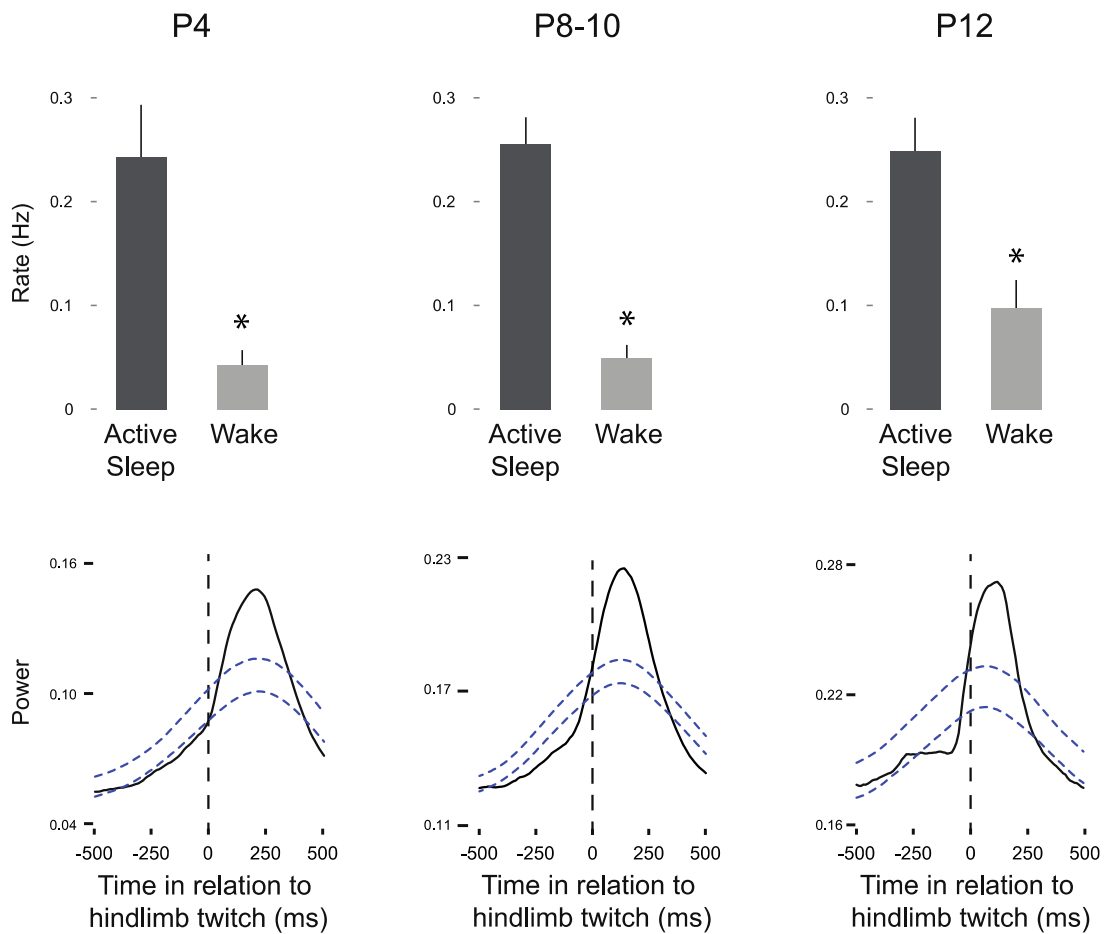
Figure 2. The hindlimb region of M1 exhibits more activity during active sleep than during wake across the early postnatal period in rats. Top row: Mean (+ SEM) rate of spindle bursts (P4: n = 6; P8-10: n = 11; P12: n = 6). * Significant difference from other group, p < .05. Bottom row: Waveform averages depicting occurrence of spindle bursts in relation to hindlimb twitches for data pooled across all subjects at each age (P4: 1172 twitches; P8-10: 4047 twitches; P12: 789 twitches). The blue dashed lines denote upper and lower acceptance bands (p < 0.05). The P8-10 data are the same as those presented in Figures 1D and 1E.
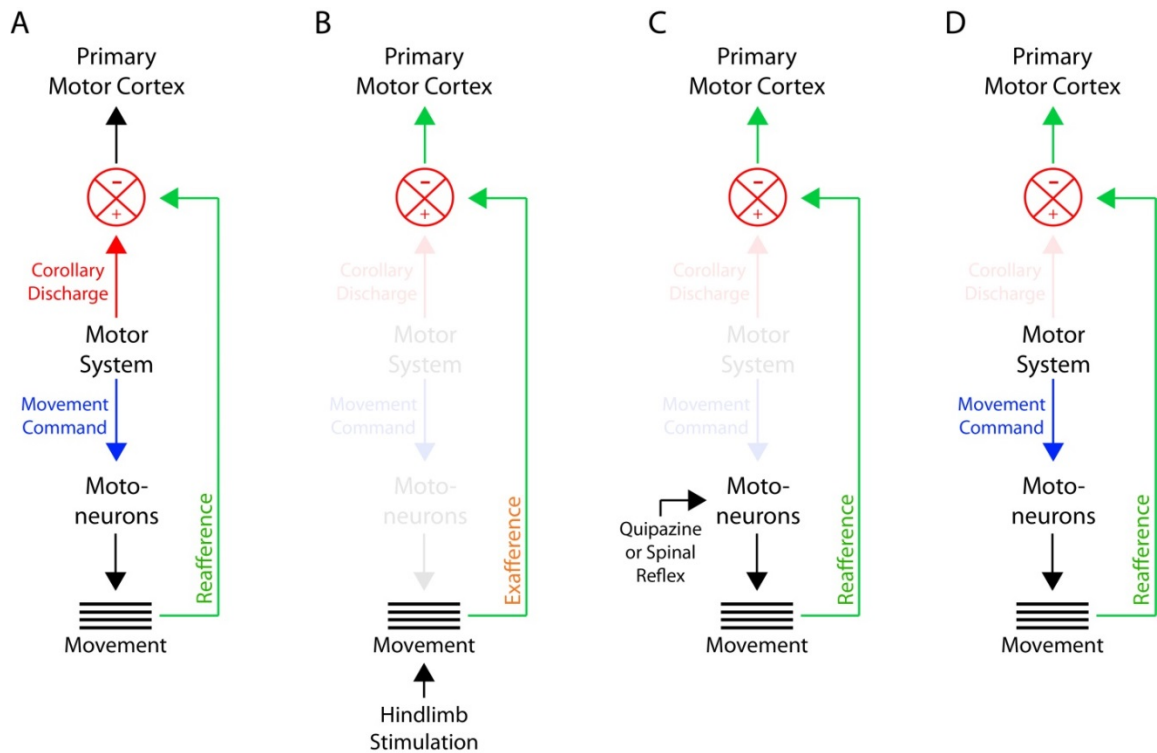
Figure 3. Schematic representation of mechanisms involved in conveying reafferent and exafferent signals to M1. (A) Conventional model depicting corollary discharge modulation of reafference for self-generated movements. Motor systems generate a descending movement command simultaneously with an ascending corollary discharge. Reafference from a moving limb is modulated by the corollary discharge signal before being conveyed to M1. When corollary discharge accurately predicts reafference, the signals can cancel each other out such that no signal is conveyed to M1, as observed here for waking movements. (B) Conventional model depicting exafference after hindlimb stimulation. No corollary discharge is generated because exafference is not self-produced. Thus, the exafference is conveyed to M1 without modification. (C) Model depicting two experimental manipulations used here to produce "unexpected" self-generated hindlimb movements. Both quipazine administration and local triggering of a

spinal reflex are presumed to have produced their effects on hindlimb movements downstream of the corollary discharge mechanisms involved in modulating M1 activity. Thus, the reafferent signals are conveyed to M1 without modification. (D) Proposed model for the neural network involved in the production of twitches and the associated processing of reafference. According to this model, the brainstem mechanisms that trigger twitches do not generate corollary discharge or, alternatively, corollary discharge is generated but its effects are somehow inhibited. Regardless, reafference is conveyed to M1 in a fashion that is similar to exafference.
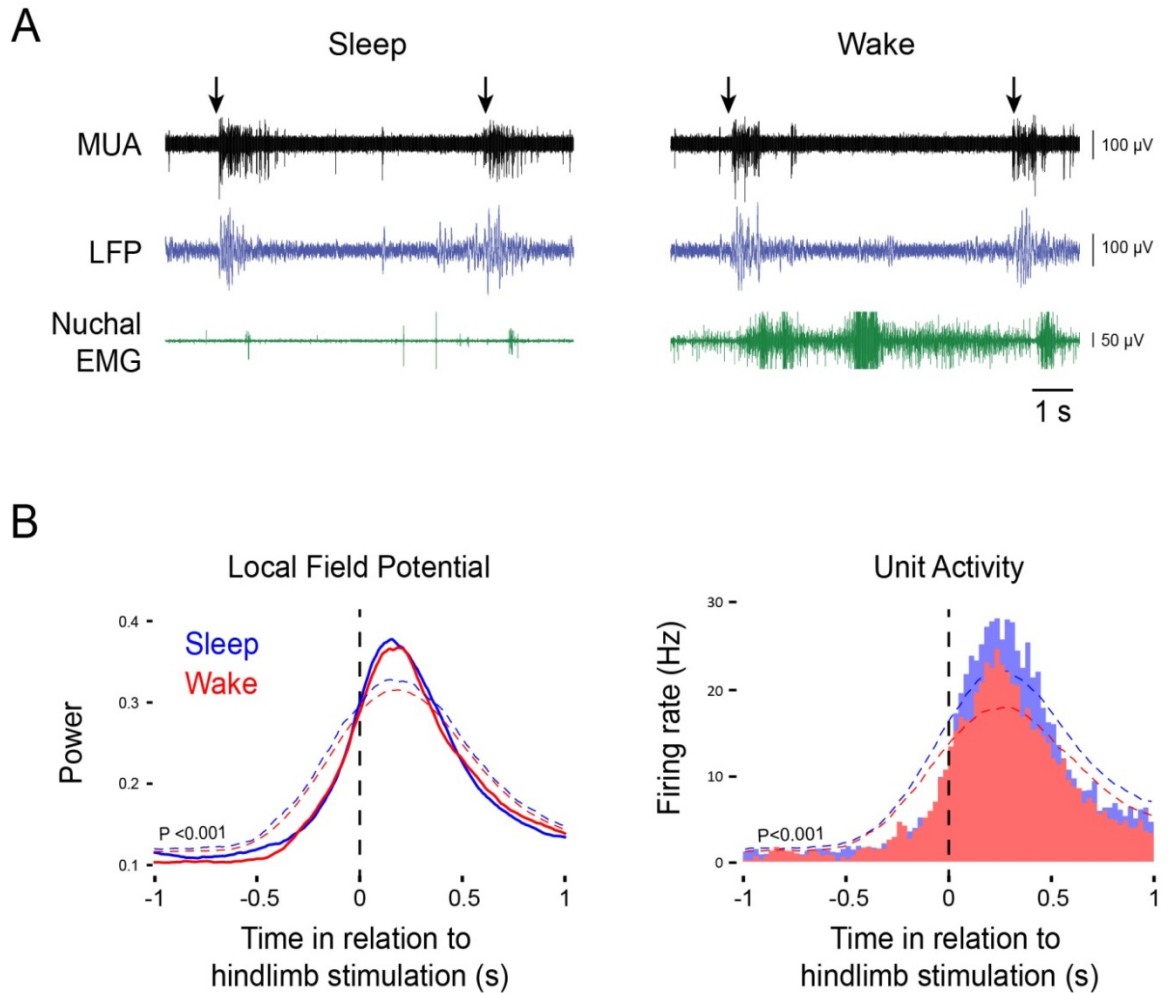
Figure 4. **Exafferent hindlimb stimulation triggers M1 activity regardless of behavioral state.** (A) Representative recordings in P8-10 subjects depicting multiunit activity (MUA; black traces) and local field potential (LFP; blue traces) responses to hindlimb stimulation (arrows) during sleep (left) or wake (right). Nuchal EMG (green traces) is also shown. (B) Left: Waveform averages for LFP power in relation to hindlimb stimulation during sleep (blue line) and wake (red line) for data pooled across all subjects (*n* = 11). Thresholds for statistical significance are indicated by the color-coded dotted lines. Right: Event correlations for unit activity in relation to hindlimb stimulation during sleep (blue

histogram; 417 stimulations) and wake (red histogram; 418 stimulations) for data pooled across all units (n = 17). Thresholds for statistical significance are indicated by the color-coded dotted lines.
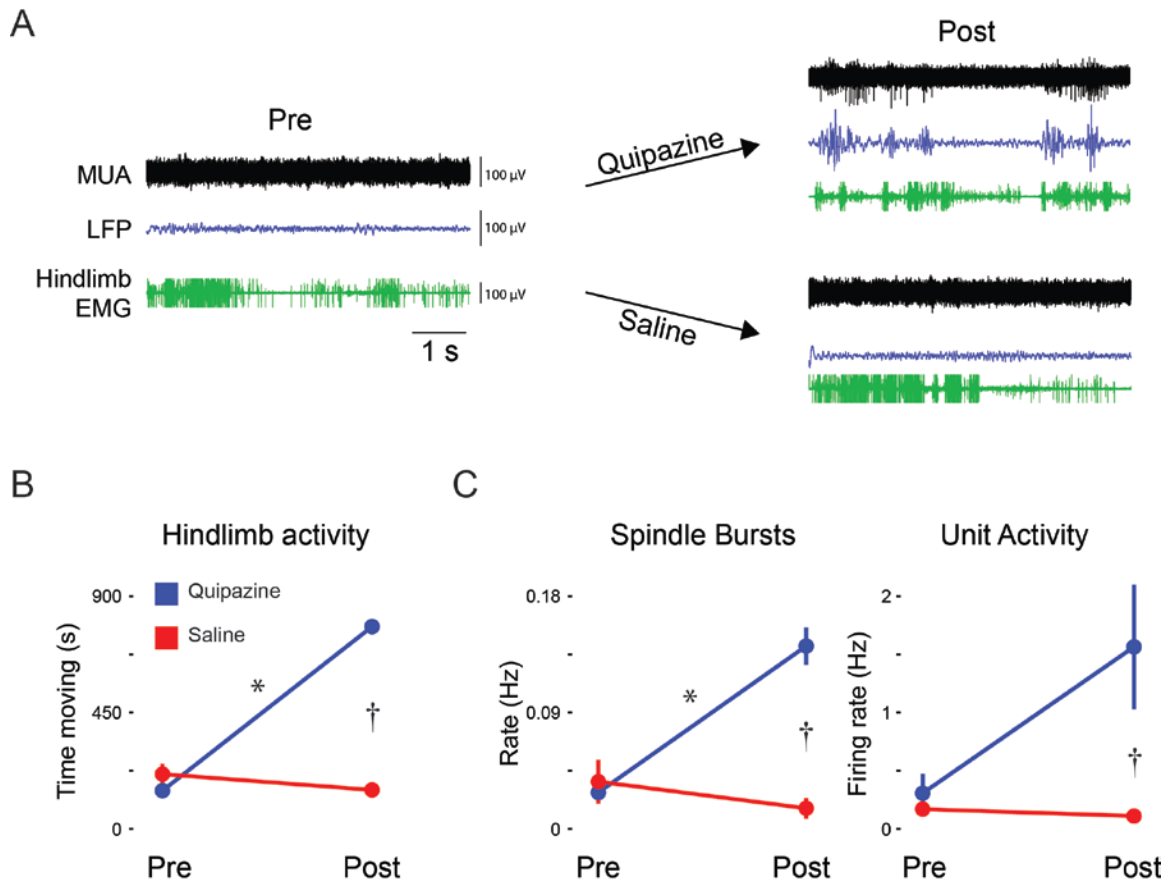
Figure 5. Pharmacological induction of hindlimb movements triggers M1 activity. (A) Representative recordings in P8-10 subjects depicting multiunit activity (MUA; black traces) and local field potentials (LFP; blue traces) before and after intraperitoneal injection of the serotonin agonist, quipazine, or saline. Hindlimb EMG (green traces) is also shown. (B) Mean ($\pm$ SEM) time that the hindlimb moved before and after quipazine or saline injection across all subjects ($n = 6$ per group). (C) Mean ($\pm$ SEM) rate of spindle bursts (left; $n = 6$ per group) and unit activity (right; $n = 4$ per group) before and after quipazine or saline injection across all subjects. * within-subjects significant difference, $p < 0.05$; † between-subjects significant difference, $p < 0.05$.
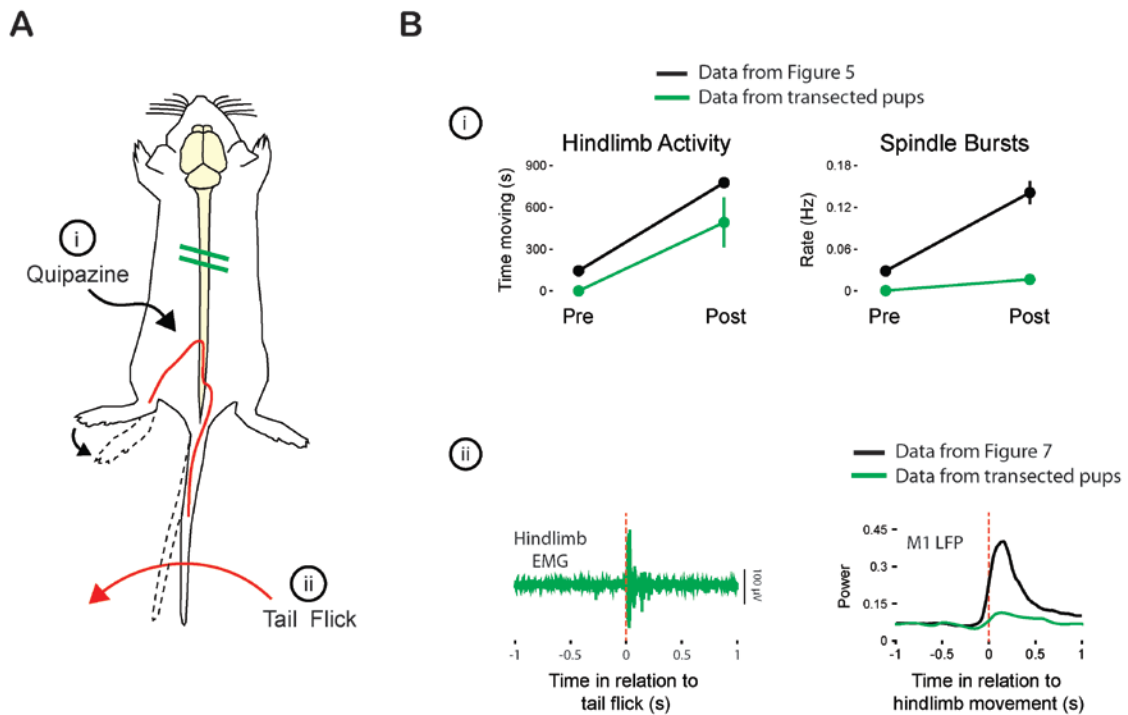
Figure 6. Effect of mid-thoracic spinal transection on hindlimb movements and M1 activity in response to (i) quipazine administration and (ii) tail flick. (A) Diagrammatic representation of the mid-thoracic transection and the two manipulations tested in P8-10 rats. (B) Top row: Mean ($\pm$ SEM) time that the hindlimb moved and the rate of spindle burst production in M1 before and after quipazine administration for data presented in Figure 5 (n = 6, black lines) and spinally transected pups (n = 2, green lines). Bottom row: Waveform averages depicting hindlimb EMG activity in the transected pups associated with the onset of reflexive hindlimb movements triggered by tail flicks. The waveform average at right compares M1 LFP activity associated with the onset of reflexive hindlimb movements triggered by tail flicks for pooled data presented in Figure 7 (n = 6,

black lines; 87 hindlimb movements) and spinally transected pups (n = 2, green

lines; 21 hindlimb movements).
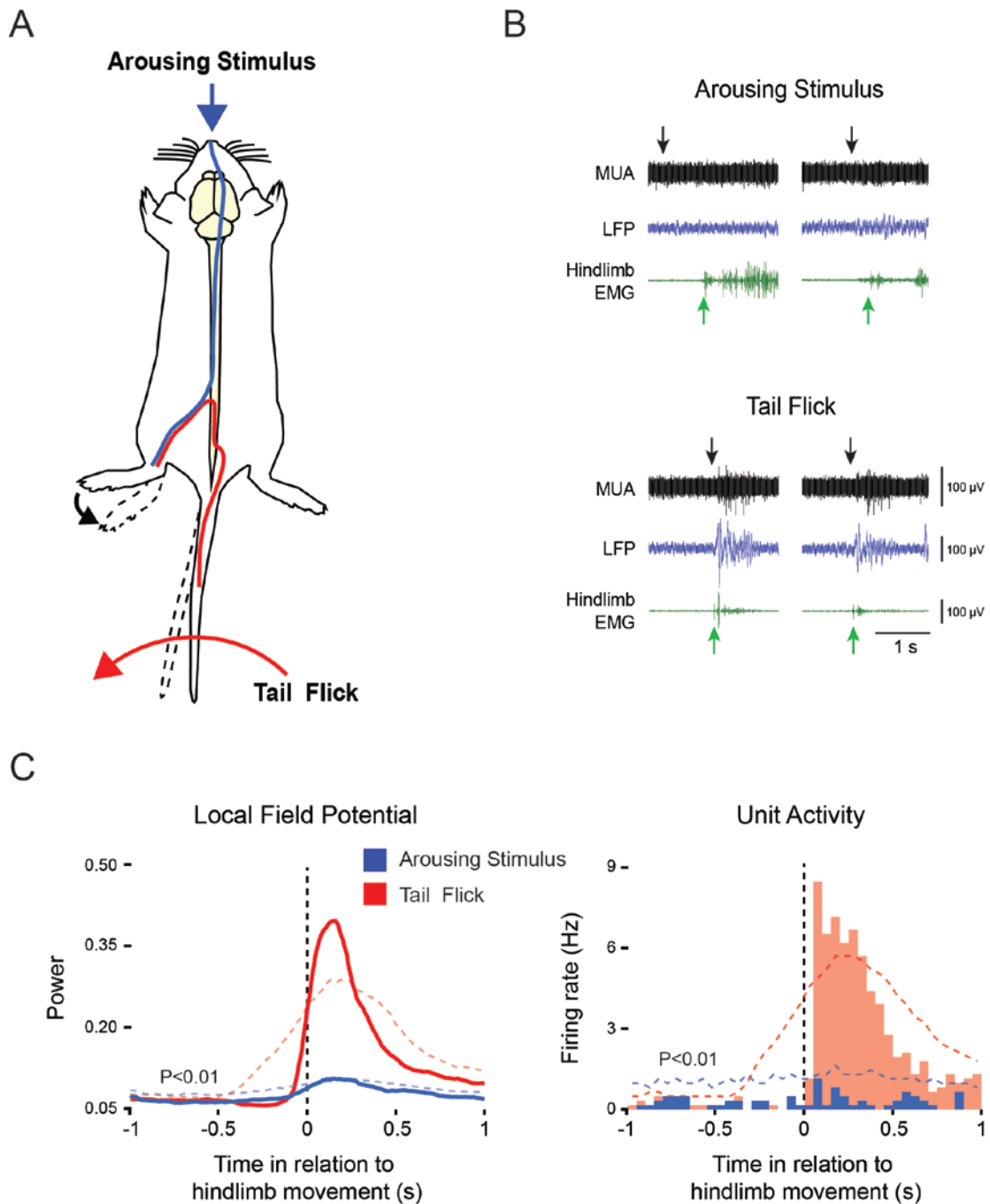
Figure 7. Effects of expected and unexpected reafference on M1 activity. (A)
Schematic diagram representing the two types of self-generated movements.
Application of a cold stimulus to the snout produced generalized arousal and
elicited vigorous hindlimb movements, thereby producing expected reafference

(blue pathway). A tail flick engaged local spinal circuits to cause a reflexive movement of the hindlimb, thereby producing unexpected reafference (red pathway). (B) Representative recordings in P8-10 subjects depicting multiunit activity (MUA; black traces) and local field potentials (LFP; blue traces) in response to the arousing stimulus (top) or tail flick (bottom). Black arrows denote stimulus presentations and green arrows denote onset of hindlimb activity. (C) Waveform averages for LFP power (left) and event correlations for unit activity (right) in relation to onset of hindlimb movement for data pooled across all animals ($n = 6$) and units ($n = 6$), respectively (arousing stimulations = 102; tail flicks = 87). Thresholds for statistical significance are indicated by the color-coded dotted lines.

CHAPTER 3: STATE-DEPENDENT GATING OF REAFFERENCE FROM SELF-GENERATED MOVEMENTS IN THE EXTERNAL CUNEATE NUCLEUS

Introduction

Animals of diverse vertebrate and invertebrate species can distinguish between sensations that arise from self-generated movements from those that arise from other-generated movements (Crapse and Sommer, 2008; Sommer and Wurtz, 2008). To make this distinction between self and other, motor areas produce copies of motor commands (i.e., corollary discharges) that are directly compared with sensory signals arising from self-generated movements (i.e., reafference; Poulet and Hedwig, 2006; Sommer and Wurtz, 2002). At the level of the neural comparator, reafference is gated or inhibited when there are no discrepancies between the corollary discharge and reafferent signals (Bell, 2001, 1989; Brooks and Cullen, 2014; Poulet and Hedwig, 2006). As a result, expected reafference arising from voluntary movements is attenuated (Haggard and Whitford, 2004; Seki et al., 2003; Voss et al., 2006), thereby increasing the salience of unexpected reafference (Brooks and Cullen, 2013; Brooks et al., 2015; Poulet and Hedwig, 2006).

In a previous study using week-old rats, we demonstrated that wake-related hindlimb movements do not trigger substantial reafference in the hindlimb region of sensorimotor cortex; in contrast, sleep-related twitches trigger robust reafference (Tiriac et al., 2014). We provided converging evidence that twitches, unlike wake movements, are processed by the nervous system as if they are

unexpected. Based on this finding, we hypothesized that the actions of corollary discharge that normally gate reafference arising from wake movements are either absent or inhibited during twitching. If so, then there must be a neural structure, located somewhere within the sensorimotor network, that acts as a comparator to specifically gate wake-related reafference. The aim of the present study was to identify a neural structure that could serve this function.

To be a comparator, a brain nucleus must integrate sensory and motor input for processing of reafferent and corollary discharge signals, respectively (Hantman and Jessell, 2010; Poulet and Hedwig, 2007; Sawtell, 2010). One possible comparator for the hindlimbs is Clarke's column, a spinal nucleus that receives primary sensory afferents from hindlimb muscle spindles as well as inputs from motor-related areas (Hantman and Jessell, 2010). However, because Clarke's column is located within the spinal cord, it is difficult to record its neural activity across sleep and wake states. In contrast, the forelimb homologue of Clarke's column—the external cuneate nucleus (ECN)—is more accessibly located in the caudal brainstem, thus allowing us to investigate its role as a comparator of forelimb corollary discharge and reafferent signals.

The ECN receives primary proprioceptive input from muscles of the forelimbs and neck and conveys sensory information to downstream structures including the cerebellum, thalamus, and cerebral cortex (Boivie and Boman, 1981; Campbell et al., 1974; Cooke et al., 1971; Huang et al., 2013; Mackie et al., 1999). In addition, the ECN receives inputs from premotor structures that are potential sources of corollary discharge. For example, the red nucleus, which

contributes to the production of wake movements and twitches in infant and adults rats (Del Rio-Bermudez et al., 2015; Li, 2015) projects to the ECN (Edwards, 1972; Holstege and Tan, 1988; Martin et al., 1974), as do the C3-C4 propriospinal neurons (PNs; Pivetta et al., 2014); the function of these projections has not been established. One possibility is that the outputs from these premotor areas are directly or indirectly responsible for the known GABAergic and glycinergic projections to the ECN, which could be involved in gating sensory input (Galindo et al., 1967; Heino and Westman, 1991; Sato et al., 1991), perhaps through presynaptic inhibition (Andersen et al., 1964; Seki et al., 2003). Moreover, the lateral reticular nucleus receives similar inputs from the PNs, and these projections have been implicated in the conveyance of corollary discharge (Alstermark et al., 2007; Azim et al., 2014; Pivetta et al., 2014).

Here, we first demonstrate that the forelimb region of sensorimotor cortex, like the hindlimb region (Tiriac et al., 2014), is selectively activated by reafference from twitches but not wake movements. This extension of our earlier findings from the hindlimbs to the forelimbs provided the foundation for investigating the role of the ECN in gating forelimb reafference. Next, recording from the ECN, we show that it exhibits an activity profile that is similar to that of sensorimotor cortex. Then, by blocking GABAergic and glycinergic receptors in the ECN, we test the hypothesis that the ECN selectively gates wake-related reafference. We show that blockade of inhibitory inputs to the ECN unmasks wake-related reafference, but has no effect on twitch-related reafference.

All together, our findings demonstrate that wake-related—but not twitch-related—reafference is gated within the ECN by GABAergic/glycinergic projections. This inhibitory control appears to be active during wake movements and absent during twitching. These findings are consistent with our hypothesis that wake-related reafference is gated when it is expected. As a further test of this hypothesis, we attached a weight to the forelimb to produce unexpected reafference during wake; as predicted, the addition of a weight produced newfound reafferent activity during wake movements. All together, these results provide the first-ever demonstration of a neural structure that acts as a state-dependent comparator of planned and performed action.

Experimental procedures

All experiments were carried out in accordance with the National Institutes of Health Guide for the Care and Use of Laboratory Animals (NIH Publication No. 80-23) and were approved by the Institutional Animal Care and Use Committee of the University of Iowa.

Subjects

A total of 42 Sprague-Dawley Norway rats (*Rattus norvegicus*) were used at P8-10. Males and females were used and littermates were always assigned to different experimental groups. Litters were culled to 8 pups within 3 days of birth. Mothers and their litters were housed in standard laboratory cages (48 x 20 x 26

cm). Food and water were available *ad libitum*. All animals were maintained on a 12:12 light-dark schedule with lights on at 0700 h.

Surgery

Head-fix preparation. For all studies, pups were prepared for testing using methods similar to those described previously (Blumberg et al., 2015, 2013a; Del Rio-Bermudez et al., 2015; Sokoloff et al., 2015a; Tiriac et al., 2012). Under isoflurane anesthesia, bipolar electrodes (50 µm diameter; California Fine Wire, Grover Beach, CA) were implanted into the *biceps brachii* muscle of the forelimb, the *extensor digitorum longus* muscle of the hindlimb, and the nuchal muscle. The skin overlying the skull was removed and a custom-built head-fix apparatus was attached to the skull with cyanoacrylate adhesive. A small hole was drilled over the forelimb region of primary sensorimotor cortex (S1 Forelimb, coordinates in relation to bregma: AP: 1 mm, L: 1.3-1.8 mm, DV: 0.5-0.8 mm) or over the external cuneate nucleus (ECN, coordinates in relation to lambda: AP: -3 mm, L: 1.6 mm, DV: 3.5-4 mm, angle of electrode: 14° directed caudally). After surgery, the pup was transferred to a humidified incubator maintained at thermoneutrality (35 ^{o}C) to recover for at least 1 h, after which it was transferred to a stereotaxic apparatus. The pup's torso was supported on a narrow platform such that the limbs dangled freely on both sides. The pup acclimated for at least 1 additional h before recordings began, by which time it was cycling between periods of sleep and wake.

For the limb-weighting experiment, a thin layer of collodion was applied to the lateral region of both forelimbs between the wrist and elbow.

Electrophysiological Recordings

The EMG electrodes were connected to a differential amplifier (A-M Systems, Carlsborg, WA; amplification: 10,000x; filter setting: 300-5000 Hz). To record from forelimb S1, 16-channel silicon depth electrodes were used (100 µm vertical separation; NeuroNexus, Ann Arbor, MI). To record from the ECN, 4-channel silicon depth electrodes were used (50 µm vertical separation; NeuroNexus, Ann Arbor, MI). Silicon electrodes had impedances ranging from 1-4 MΩ. To simultaneous perform ECN recordings during iontophoretic application of GABA and glycine receptor antagonists, multibarrel electrodes were used (Carbostar-3; Kation Scientific, Minneapolis, MN). Electrodes were connected to a headstage which communicated with a data acquisition system (Tucker-Davis Technologies, Alachua, FL) that amplified (10,000x) and filtered the signals. All recordings in S1 were obtained using a 0-5000 Hz band-pass filter and all recordings in ECN were obtained using a 500-5000 Hz band-pass filter. A 60 Hz notch filter was also used. Neurophysiological and EMG signals were sampled at 25 kHz and 1 kHz, respectively, using a digital interface and Spike2 software (Cambridge Electronic Design, Cambridge, UK).

Prior to insertion of the silicon probe into S1 or ECN, the electrode surface was coated with fluorescent DiI (Life Technologies, Carlsbad, CA) for subsequent histological verification of electrode placement. A Ag/AgCl ground electrode

(Medwire, Mt. Vernon, NY, 0.25 mm diameter) was placed into the visual cortex ipsilateral to the silicon probe. Brain temperature was monitored using a fine-wire thermocouple (Omega Engineering, Stamford, CT) placed in the visual cortex contralateral to the ground wire. For all experiments, brain temperature was maintained at 36-37 °C.

Electrode position was established when it was possible to reliably evoke neural activity by gentle stimulation of the contralateral (for sensorimotor cortex) or ipsilateral (for ECN) forelimb. Other parts of the body were also stimulated to confirm selectivity. Using procedures similar to those described previously (Del Rio-Bermudez et al., 2015; Sokoloff et al., 2015a; Tiriac et al., 2012), data acquisition began after local field potentials (LFP) and multiunit activity (MUA) were identified and had stabilized for at least 10 min.

Experimental Procedure

Spontaneous activity during sleep and wake. We recorded spontaneous neural activity in cycling unanaesthetized infant rats (n = 6 for S1 recordings, n = 14 for ECN recordings). Recording sessions comprised continuous collection of neurophysiological and EMG data for at least 30 min. During acquisition, an experimenter monitored the subject's behavior and digitally marked the occurrence of sleep-related twitching and wake movements in synchrony with the physiological data. For the digital marking of limb movements, we used two sets of markers. One set of digital markers was used for forelimb twitches and wake movements, and another set was used for twitches and wake movements of all

limbs. As described elsewhere (Karlsson et al., 2005), myoclonic twitches are phasic, rapid, and independent movements of the limbs and tail against a background of muscle atonia; in contrast, wake movements, which are high-amplitude, coordinated movements occurring against a background of high muscle tone, include locomotion, stretching, and yawning. Finally, the experimenter was always blind to the physiological data when scoring behavior.

Limb-weight manipulation. In 12 head-fixed P8-10 rats, S1 forelimb activity was recorded during a 15-min baseline period ("pre-weight"). At the end of this baseline period, a weight was attached to the collodion on the lateral side of the contralateral forelimb ("weight" period). For the experimental group, the weight had a mass equal to 100% of the forelimb weight (for a 25 g P10 pup, forelimb weight is equal to 1 g). For the control group, the weight had a mass that was 10% of the forelimb weight. At the end of the 45-min weight period, the weight was removed and cortical activity was recorded for another 45 minutes ("post-weight" period)

Forelimb stimulation. In 6 of the 14 animals in which spontaneous sleep-wake activity was recorded in the ECN, the forelimb ipsilateral to the recording site was stimulated using a fine paintbrush over a period of 10 min. The brush was applied to the base of the paw and the limb was flexed at the elbow. The stimulations were performed similarly during sleep and wake. On average, stimulations were repeated every 5-10 s.

Iontophoretic injections of GABA and glycine receptor antagonists. In 10 head-fixed P8-10 rats, ECN activity was recorded before and during iontophoretic infusions of $GABA_A$ (10 mM bicuculline methiodide; Sigma-Aldrich, St. Louis, MO) and glycine (10 mM strychnine hydrochloride; Sigma-Aldrich, St. Louis, MO) receptor antagonists or saline. Before infusion, 30 min of baseline ECN activity was recorded. During this recording, a -10 nA retaining current was used to ensure that the antagonists did not leak passively into the ECN. After the baseline recording, the current was switched to +50 nA to eject the drugs and another 30 min of ECN activity was recorded. After this recording period, fluorogold was injected with the same current parameter that was used for drug infusion to mark the location of the electrode.

Histology

At the end of the recording session, the pup was overdosed with sodium pentobarbital (1.5 mg/g) and perfused transcardially with phosphate buffered saline followed by 4% paraformaldehyde. Brains were sectioned at 50 µm using a freezing microtome (Leica Microsystems, Buffalo Grove, IL). Recording sites were verified by visualizing the DiI tract or the fluorogold injection at 5-20X magnification using a fluorescent Leica microscope (Leica Microsystems, Buffalo Grove, IL). Tissue slices were then stained using cresyl violet and the location of the recording site was identified.

Data Analysis

MUA and LFP analysis. All open channels (initially acquired with 0-5000 Hz band-pass filters) were filtered for multi-unit activity (500-5000 Hz). Any channels with units were processed by spike sorting in Spike2 (Cambridge Electronic Design, Cambridge, UK). For LFPs, channels were band-pass filtered (1-40 Hz) to extract spindle bursts. Spindle bursts were defined as comprising at least 3 oscillations, a dominant frequency of 10-15 Hz, and a duration of at least 100 ms (Khazipov et al., 2004). LFP channels were converted using root mean square (RMS) with a time constant of 0.01 s. Five random high-amplitude spindle bursts were averaged and the baseline value of the RMS channel was calculated. The midpoint between those two values was used as a threshold for identification of spindle bursts. A second pass through the data was performed to manually remove any spindle bursts that did not match the requisite criteria. Throughout this process, artifacts in the LFP and MUA signals were identified and manually removed.

Identification of behavioral state and motor activity. Sleep and wake periods were defined using methods described previously (Karlsson et al., 2005; Tiriac et al., 2012). Briefly, the nuchal EMG signal was dichotomized into periods of high tone (indicative of wake) and atonia (indicative of sleep). Active sleep was characterized by the occurrence of myoclonic twitches against a background of muscle atonia (Seelke and Blumberg, 2008). Spikes of EMG activity with amplitudes greater than 3x baseline were considered twitches.

For the identification of forelimb wake movements, the forelimb EMG was rectified and smoothed (0.01 ms). To be considered a wake movement, a spike in the forelimb EMG had to be at least 300 ms in duration and had to occur while nuchal muscle tone was high (indicative of wakefulness). Five random wake movements that met these criteria were selected and their maximum amplitude was averaged. Using the midpoint between atonia and max amplitude of wake movements as a threshold, an automatic peak detection was applied to extract forelimb movements as events. Similar to spindle burst detection, a second pass through the data was performed to manually remove any wake movements that did not match the requisite criteria.

Analysis of state dependency. There were at least 20 bouts of wake and active sleep for each pup. Across these bouts, the mean rates of spindle burst production and unit activity were determined. First, for each individual pup, successive bouts of wake and active sleep were treated as pairs and the Wilcoxon matched-pairs signed-ranks test (SPSS, IBM, Armonk, NY) was used to test for differences in rates of spindle burst production and unit activity between the two states. Second, the mean rates of spindle burst production and unit activity during wake and active sleep were calculated for each pup and compared within each age group using paired *t* tests.

Event correlations and waveform averages for S1 and ECN activity triggered by twitches. The relationship between twitches and S1 and ECN activity was

assessed as follows: First, the data for all pups were concatenated into one file. From this file, using twitches as triggers, event correlations (for S1: 1000-ms windows, 25-ms bins; for ECN: 300-ms windows, 1-ms bins) of unit activity and waveform averages of spindle activity were constructed. We tested statistical significance for both event correlations and waveform averages by jittering twitch events 1000 times within a 500-ms window using the interval jitter parameter settings within PatternJitter (Amarasingham et al., 2012; Harrison and Geman, 2009) implemented in Matlab (MathWorks, Natick, MA). We corrected for multiple comparisons using the method of Amarasingham et al. (Amarasingham et al., 2011); this method produces upper and lower confidence bands (p < .01) for each event correlation and waveform average.

Effects of forelimb weighting on forelimb S1 LFP and MUA activity. For each animal in each group, LFP traces were filtered for spindle activity and single units were extracted using the same methods described above. Forelimb twitch and wake movements were also extracted as discrete events. Next, each animal's recording was divided into seven 15-min time periods. In chronological order, these periods consisted of pre-weight, weight (W1-3) and post-weight (PW1-3) periods. For each time period and for each behavioral state, waveform averages (1000-ms windows) and event correlations (1000-ms window, 10-ms bins) were generated to correlate LFP and MUA activity, respectively. Brain activity was triggered on contralateral forelimb twitches or wake movements.

To normalize the waveform averages for each pup, mean LFP power during quiescence (1-1.5 s preceding motor activity) was first calculated. These means were then subtracted from each respective waveform average. Next, the waveform average during the "pre-weight" period was subtracted from the waveform averages of all other time periods (W1 through PW3; see Figure 12). Peak LFP power for each waveform average was then calculated. Peak LFP power across the 6 time periods (W1 – PW3) was compared using repeated-measures ANOVAs performed. When interactions were significant, follow-up repeated-measures and one-way ANOVAs were used, as appropriate.

To normalize the event correlations for each pup, mean firing rate during quiescence (1-1.5 s preceding motor activity) was first calculated. These means were then subtracted from each respective event correlations. Next, the event correlations during the "pre-weight" period was subtracted from the event correlations of all other time periods (W1 through PW3; see figure 12).

Stimulus-triggered event correlations and waveform averages. The 10-min recordings from the forelimb stimulation trials were divided into periods of sleep and wake. Perievent histograms (500-ms windows, 10-ms bins) were constructed using onset of EMG activity produced by forelimb stimulations as the trigger. Average peak firing rate across all stimulations for each behavioral state was determined. Peak firing rate was compared using a paired t test.

Effects of GABA and glycine receptor antagonists on ECN neural activity. For each animal in each group, recordings were divided into a pre- and post-infusion period (30 min each). For each time period and for each behavioral state, event correlations (3000-ms windows, 50-ms bins) were generated to correlate MUA activity to ipsilateral forelimb twitches and wake movements. For each event correlation, mean firing rate during quiescence (1-1.5 s preceding motor activity) was calculated. These means were then subtracted from each respective event correlation. For each animal, the event correlation of the pre-infusion time period was subtracted from the event correlation of the post-infusion time period. The resulting event correlations depicting the change in firing rate (Δ firing rate) were then averaged within each experimental group for each behavioral state and standard errors for every bin was calculated. Peak change in firing rate around the expected latency of sensory reafference was then calculated along with standard errors. Experimental groups within each behavioral state were compared using a paired t-test. Expected latency was determined using the raw event correlation for wake (Figure 10C, left) and sleep (Figure 10D).

The frequency of wake movements, twitches, and action potentials across the two time periods were calculated. Statistical significance between time periods was determined using paired t tests. For each of the measurements above, the percent difference between the pre- and post-infusion time periods was also calculated. Statistical significance between experimental groups was determined using an independent samples t test.

Unless otherwise noted, alpha was set at 0.05 and Bonferroni corrections were applied when appropriate.

Results

Twitch-related, but not wake-related, movements trigger reafference in S1

We recorded neural activity in the forelimb region of sensorimotor cortex (S1) to establish if it, like the hindlimb region (Tiriac et al., 2014), exhibits state-dependent neural activity. Unanesthetized and head-fixed 8- to 10-day-old rats cycled spontaneously between sleep and wake with their limbs dangling freely. Recording from the forelimb region of S1, we characterized reafference arising from self-generated sleep and wake movements. Figure 8A depicts representative spindle bursts recorded from the local field potential (LFP) and multiunit activity (MUA) in relation to both wake movements and twitches. Spindle bursts and MUA were particularly prominent during periods of twitching and were virtually absent during periods of wake movements. Across all pups, the mean rate of spindle bursts (t_5 = 10.2, p < 0.01, n = 6 pups) and unit activity (t_7 = 3.9, p < 0.01, n = 8 units) was significantly higher during active sleep than during wake (Figure 8B). Moreover, LFP power and unit activity were triggered by forelimb twitches with a latency of 100-125 ms (Figure 8C). These results confirm that the forelimb and hindlimb regions of S1 exhibit similar state-dependent gating of reafference in response to forelimb and hindlimb movements, respectively.

Twitch-related, but not wake-related, movements trigger reafference in the ECN

If the ECN is a comparator of reafference and corollary discharge signals, then it should exhibit state-dependent activity that is similar to that of S1. We recorded neural activity in the caudal region of the ECN in P8-P10 rats as they cycled between sleep and wake (Figure 9A). The caudal region of the ECN has a strong forelimb representation (Campbell et al., 1974). Consistent with this, ECN firing rate was higher in response to forelimb twitches than in response to hindlimb (Figure 9B; $t_8 = 3.5$, p < 0.01) or nuchal twitches ($t_{21} = 3.2$, p < 0.01). There was no significant difference in ECN firing rate between hindlimb and nuchal twitches ($t_8 = 1.3$). As expected given the relative anatomical locations of the ECN and S1, the latency to twitch-related ECN activity (10-50 ms) was shorter than that observed in S1 (100-125 ms). Importantly, and similar to S1, ECN firing rate was significantly state dependent, with greater activity occurring during periods of forelimb twitches than during periods of forelimb wake movements ($t_{15} = 2.8$, p < 0.05, Figure 9C).

It is possible that the inhibition of wake-related reafference was due to a global inhibition of all sensory activity during wakefulness. If so, then stimulation of the ipsilateral forelimb should produce less exafference in the ECN during wake than during sleep. To test for this possibility, we recorded from ECN neurons while performing ipsilateral forelimb stimulation in 6 pups. As shown in Figure 9D, there was no significant difference in ECN activity in response to sleep or wake-related stimulation ($t_5 = 1.2$). This result is consistent with the lack

of state-dependent evoked activity observed previously in sensorimotor cortex (Tiriac et al., 2014).

Disinhibition of the ECN unmasks wake-related reafference

Figure 10A depicts our proposed model to explain state-dependent modulation of reafference in the ECN. During wake movements, a motor copy to the ECN releases GABA and/or glycine, thereby gating reafference. Accordingly, we hypothesize that blockade of GABA and glycine receptors in the ECN would disinhibit wake-related reafference. In contrast, we propose that the motor copy pathway is suspended during twitching, effectively removing inhibitory input from the motor system and thereby permitting the transmission of reafferent signals beyond the ECN. Thus, we hypothesize that twitch-related reafference would be unaffected by blockade of GABA and glycine receptors. To test these hypotheses, we recorded ECN activity before and during iontophoretic infusion of a cocktail of $GABA_A$ (10 mM bicuculline methiodide) and glycine (10 mM strychnine hydrochloride) receptor antagonists or saline (Figure 10B; n = 5 pups per group). As predicted, inhibitory blockade unmasked ECN reafference in response to forelimb wake movements (t_8 = 3.7 p < 0.01, Figures 10C). Moreover, and again as predicted, inhibitory blockade had no effect on ECN reafference in response to forelimb twitches (Figures 10D). Finally, infusions of saline had no effect on either wake or sleep reafference.

In conjunction with the earlier finding that exafference is reliably evoked in the ECN regardless of state (Figure 9D), the results presented here demonstrate

that GABA/glycine inputs modulate ECN activity not just during wake, but specifically during wake movements. To affirm that the inhibitory input to the ECN conveys a motor copy and not a motor command, we determined whether inhibitory blockade of the ECN alters motor activity. Blocking GABA and glycine receptors had no effect on the amplitude of wake movements (Figure 11A), the frequency of forelimb wake movements (Figure 11B, top row), or the frequency of forelimb twitches (Figure 11B, middle row). Moreover, inhibitory blockade did not increase tonic neural activity in the ECN, thus providing further evidence that the inhibitory inputs to the ECN function specifically in the context of movement (Figure 11B, bottom row).

Wake-related activity in S1 increases when reafference is unexpected

The above findings provide mechanistic evidence that the gating of reafference during wake is due to a GABA/glycine inhibitory drive that is recruited specifically in conjunction with wake movements (Figures 10 and 11). Because the ECN receives input from motor areas, and because the gating of reafference is linked to motor activity, we hypothesized that this inhibitory drive could be reflecting the actions of a corollary discharge signal that matches expected reafference (Figure 12A). If true, then creating a mismatch between corollary discharge and reafference signals should induce increased sensory feedback during self-generated wake movements (Brooks et al., 2015) (Figure 12B, left). To create a mismatch, we manipulated reafference by attaching a heavy or light weight to the forelimb (Figure 12B, right). We hypothesized that an unexpected load to the

forelimb induces reafference that would pass through the ECN (and other structures with similar gating properties) to activate downstream sensory areas such as S1.

We used a weight that doubled the mass of the forelimb (100% forelimb weight) or increased it negligibly (10% forelimb weight). Activity in forelimb S1 was recorded for 15 min before attachment of the weight, for 45 min during limb weighting, and for another 45 min after removal of the weight. We predicted that doubling forelimb weight would increase wake-related S1 activity. Moreover, if rat pups can rapidly adapt their motor predictions, as can adult monkeys (Brooks et al., 2015), then the induced S1 activity should decrease over the 45-min period. Accordingly, removal of the weight should produce newly unexpected reafference, again resulting in increased wake-related S1 activity that would dissipate over time.

A three-factor repeated-measures ANOVA revealed a significant Time x Weight Group x Sleep-Wake State interaction ($F_{5,55}$ = 4.1, $p < 0.05$). For wake movements, ANOVA revealed a significant Time x Weight Group interaction ($F_{5,25}$ = 7.0, $p < 0.01$). Follow-up ANOVAs revealed that S1 activity increased significantly in response to forelimb wake movements immediately after the addition of the 100% weight, but not after the addition of the 10% weight (Figures 12C-D and 13). As predicted, the magnitude of the wake-related S1 activity decreased over time. Then, removal of the 100% weight again produced an immediate increase in wake-related S1 activity, which again decreased over time. It should be stressed that, with respect to these measures of S1 activity,

there was no statistical difference between attachment and removal of the forelimb weight: In both cases, S1 activity increased and then decreased back to baseline.

Because twitches already trigger abundant S1 activity, we predicted that doubling forelimb weight would not substantially alter S1 activity. Indeed, repeated-measures ANOVA failed to reveal any significant effects. Attachment and removal of the 100% weight had no discernible effect on twitch-related S1 activity (Figure 12C-D and 13).

It is possible that the diminution of wake-related S1 activity over the 45-min weighting and post-weight periods was due to sensory adaptation of peripheral receptors. If so, then we should have observed similar time-related decreases in S1 activity for wake movements and twitches. The fact that twitch-related S1 activity did not diminish over time argues against this possibility. All together, these findings are consistent with the hypothesis that reafference from wake movements, but not twitches, is modulated by corollary discharge signals.

Discussion

The ECN as a neural comparator of planned and performed actions

In a previous study, we provided converging evidence that twitches, unlike wake movements, robustly activate the sensorimotor system because they are processed as if they are unexpected (Tiriac et al., 2014). That earlier study did not identify a neural mechanism that could explain that effect. Here we identify the ECN as a neural comparator that exclusively gates reafference associated

with wake movements; this neural mechanism is not engaged during twitching. To our knowledge, this is the first report of a neural comparator that is state-dependently modulated.

To establish that the ECN is a comparator of corollary discharge and reafferent signals, several criteria must be met (Poulet and Hedwig, 2007). First, to be a comparator the ECN must be a sensory structure. Indeed, the ECN processes proprioceptive inputs from forelimb and nuchal muscles (Campbell et al., 1974). Moreover, recordings from anesthetized cats have demonstrated that the ECN codes, with high fidelity, the precise stretch on muscle fibers (Mackie et al., 1999).

Second, the ECN should receive motor-related input. In fact, the ECN receives direct and indirect input from areas that control motor behavior. Two such areas are the premotor PNs in the C3-C4 region of spinal cord (Pivetta et al., 2014) and the red nucleus in the brainstem (Edwards, 1972; Holstege and Tan, 1988; Martin et al., 1974). Although the function of these projections to the ECN is unknown, it should be noted that the PNs (and perhaps also the red nucleus via the PNs) convey corollary discharge signals to another medullary structure, the lateral reticular nucleus (Alstermark et al., 2007; Azim et al., 2014; Pivetta et al., 2014).

Third, to be a comparator, the ECN should not participate in the production of movement. As shown here, disinhibition of the ECN had no discernible effect on the production of wake movements or twitches (Figure 11).

Finally, and most critically, a comparator must gate reafference arising from movements. The ECN clearly possesses this function as inhibitory blockade of this structure unmasked reafference exclusively during wake movements (Figure 10C). Importantly, inhibitory blockade had no effect on the ECN's tonic firing rate (Figure 11B, bottom row), thus demonstrating that inhibitory control of the ECN is not engaged indiscriminately throughout the waking state. Furthermore, when we manually stimulated the forelimbs, ECN activity was evoked similarly during sleep and wake (Figure 9D).

To summarize, the ECN receives sensory input from the forelimbs, receives motor-related inputs from PNs and red nucleus, is not involved in the production of motor behavior, and specifically gates reafference from wake-related movements. All together, these findings converge on the conclusion that the ECN is a neural comparator of planned and performed actions during wakefulness.

The ECN exclusively gates expected reafference

Inhibition of sensory reafference can take two forms. In chirping crickets, for example, corollary discharges inhibit all auditory sensations, whether caused by self-generated chirps or external auditory stimuli (Poulet and Hedwig, 2006). This type of gating prevents desensitization of auditory receptors but lacks the ability to discriminate discrepancies between corollary discharge and reafferent signals. Alternatively, when primates make voluntary head movements, corollary discharge signals specifically inhibit *expected* reafference; in contrast, during

voluntary movements with an unexpected load applied to the head, reafference is not completely inhibited (Brooks et al., 2015). Similar to primates, we show here that an unexpected load applied to the forelimb results in increased S1 activity during wake-related forelimb movements (Figures 12C-D and 13) that may reflect a mismatch between corollary discharge and reafference signals.

The increase in wake-related reafference that followed attachment of the weight diminished over time, only to increase again upon removal of the weight. As in adult primates (Brooks et al., 2015), such findings can be interpreted as resulting from the updating of an internal model that rapidly transforms an unexpected stimulus into an expected one (Franklin and Wolpert, 2011). After 45 min with the weight attached, it is now the removal of the weight that triggered unexpected reafference during wake movements.

The models in Figures 10A and 12B are likely lacking components that contribute to the modulation of reafferent signaling. For example, in addition to the alpha motor system that directly activates muscle fibers, the gamma motor (or fusimotor) system maintains dynamic tension on muscle spindles (for review, Proske and Gandevia, 2012). In adult cats, the fusimotor system appears inhibited during AS (Kubota and Tanaka, 1968) and larger reafferent responses can occur when the fusimotor system is not engaged than when it is engaged (Wise et al., 1999). Thus, it is possible that twitches and wake movements differentially engage the fusimotor system, perhaps contributing to the finding that limb weighting had no discernible effect on twitch-related reafference.

Resolving the functions of the fusimotor system will likely enhance our understanding of the ECN's role as a neural comparator.

The capacity to effectively gate expected reafference is typically attributed to the action of internal models (Cullen, 2004; Wolpert et al., 1998). The action of such a model could be invoked to explain our limb-weighting experiment: Specifically, the increased forelimb weight produced a temporary mismatch between expectancy and reafference and this mismatch disappeared as the internal model was updated (see Brooks et al., 2015). If this account is correct, our findings suggest that engagement of the internal model, at least with regard to sensory gating, occurs predominantly during wake movements. In broader context, then, our results imply that wake movements emphasize feedforward control and twitches emphasize sensory feedback. Such a distinction should not be interpreted to mean that motor copies are not produced in conjunction with twitches. On the contrary, it is likely that both twitches and wake movements are associated with multiple loops of corollary discharge mechanisms across the neuraxis, with each loop contributing in different ways to the functional control and maintenance of the sensorimotor system (Crapse and Sommer, 2008).
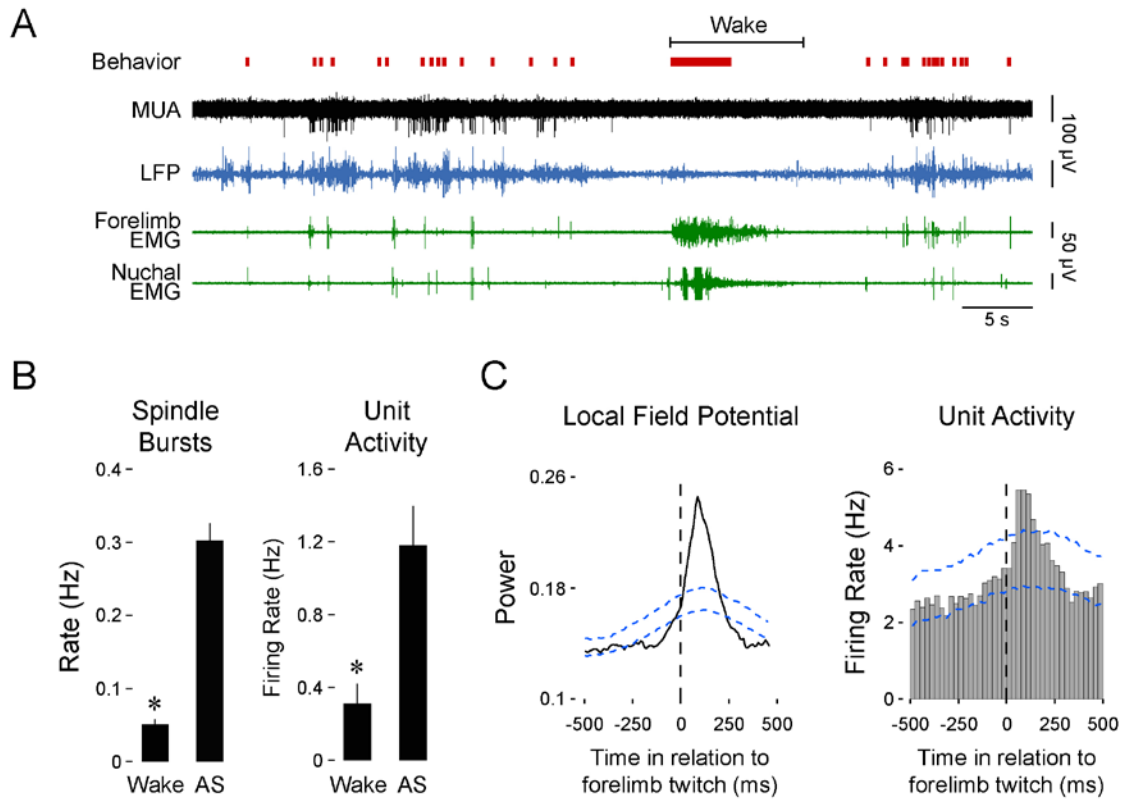
Figure 8. Forelimb twitches, but not wake movements, trigger neural activity in forelimb sensorimotor cortex. (A) Representative data depicting sleep and wake behavior, MUA, LFP, and forelimb and nuchal EMG during spontaneous sleep-wake cycling. Red tick marks denote forelimb twitches and red horizontal bars denote forelimb wake movements as scored by the experimenter. (B) Mean (+SEM) rate of spindle burst (n = 6 pups) and unit activity (n = 8 units) during periods of wake and active sleep. * significant difference from active sleep, p < 0.05. (C) Waveform average and event correlation for LFP power and unit activity, respectively, in relation to forelimb twitches (2413 and 2943 twitches, respectively). The blue dashed lines denote upper and lower acceptance bands (p < 0.05).
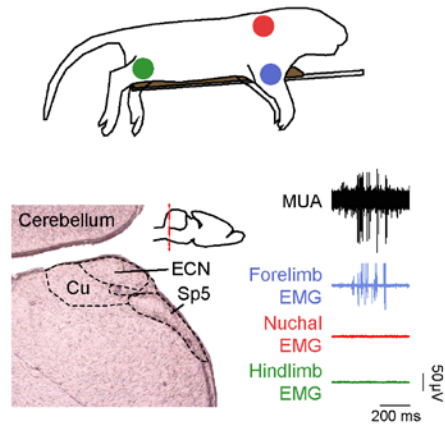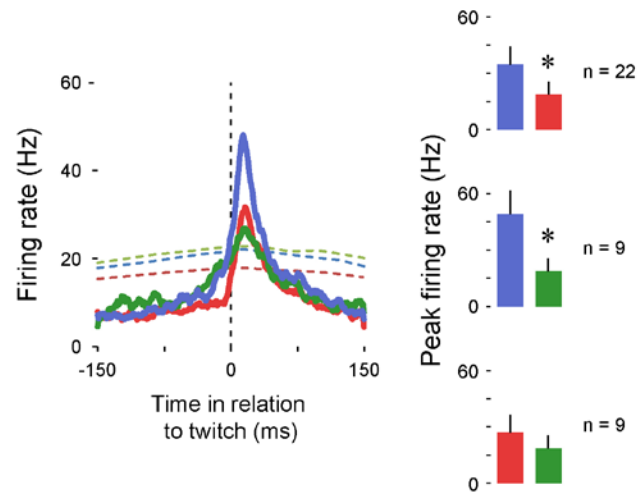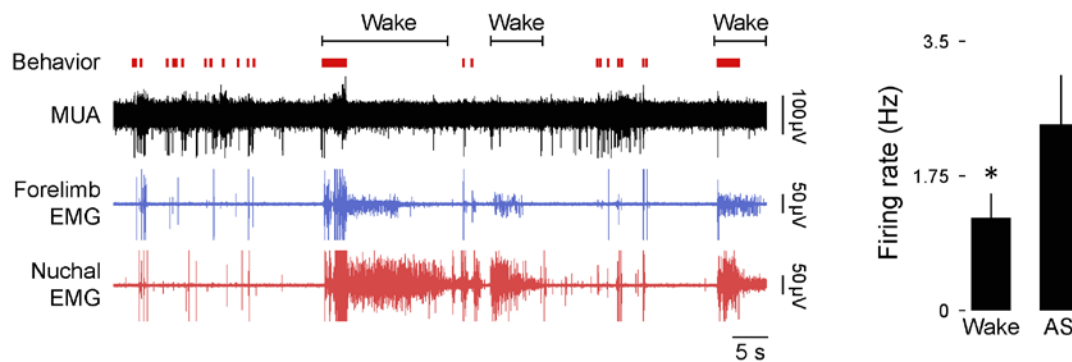
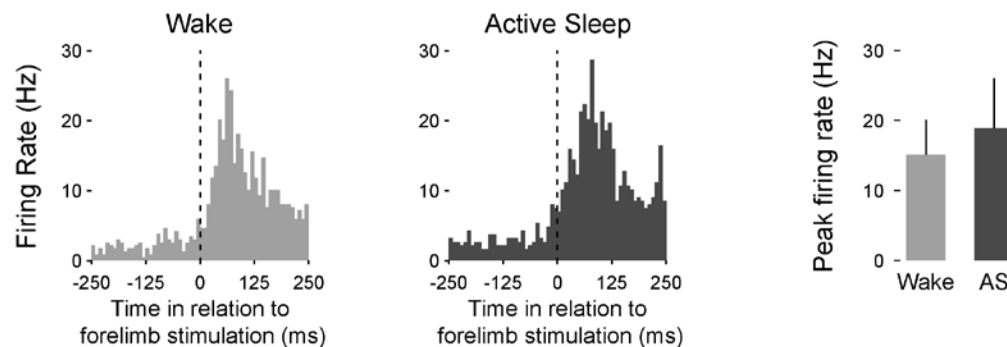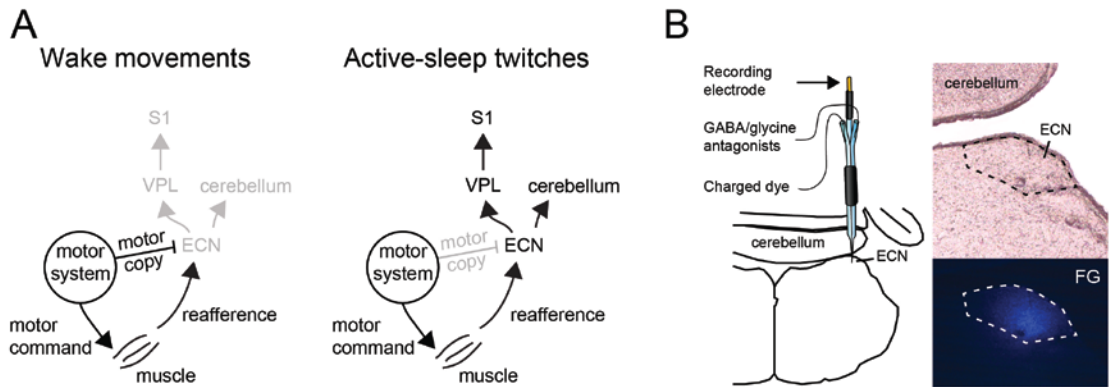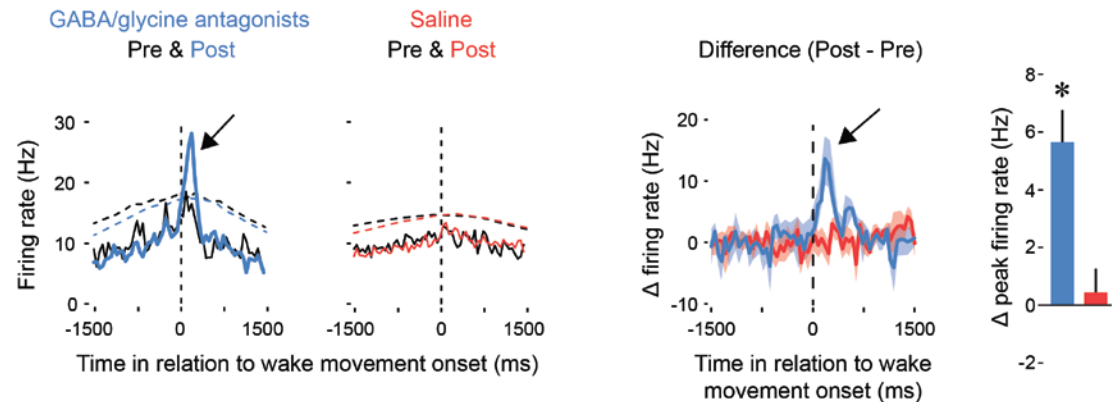**Figure 9. The ECN exhibits wake-dependent inhibition of sensory reafference.** (A) Top: For all ECN recordings, P8-P10 rats were instrumented with forelimb (blue) and nuchal (red) EMGs (n = 22). A subset of these rats also

had a hindlimb (green) EMG (n = 9). The torso was supported by a platform and the limbs dangled freely. Bottom left: Coronal brain section depicting the anatomical location of the ECN in the hindbrain (inset; red dashed line depicts AP position of the coronal section). Bottom right: Sample record of a burst of ECN reafference in response to forelimb twitches. (B) Left: Event correlations for unit activity in relation to forelimb (blue), nuchal (red), and hindlimb (green) twitches. The colored dashed lines denote upper acceptance bands (p < 0.05) for the event correlations. Right: Pairwise comparisons of mean (+SEM) peaks in unit activity (Hz) in response to forelimb, nuchal, and hindlimb twitches. Comparisons are between forelimb and nuchal muscles (top), forelimb and hindlimb muscles (middle), and nuchal and hindlimb muscles (bottom). (C) Left: Representative data depicting sleep and wake behavior, MUA, and forelimb and nuchal EMG during spontaneous sleep-wake cycling. Red tick marks denote forelimb twitches, and red horizontal bars denote forelimb wake movements as scored by the experimenter. Right: Mean (+SEM) unit activity (n = 16) during wake and active sleep periods. * significant difference from active sleep, p < 0.05. (D) Left: Event correlations for evoked unit activity in response to forelimb stimulations performed during active sleep (n = 188 stimulations) and wake (n = 238 stimulations) across 6 ECN units in 6 pups. Right: Mean (+SEM) peak unit activity (n = 6) derived from event correlations during wake and active sleep.
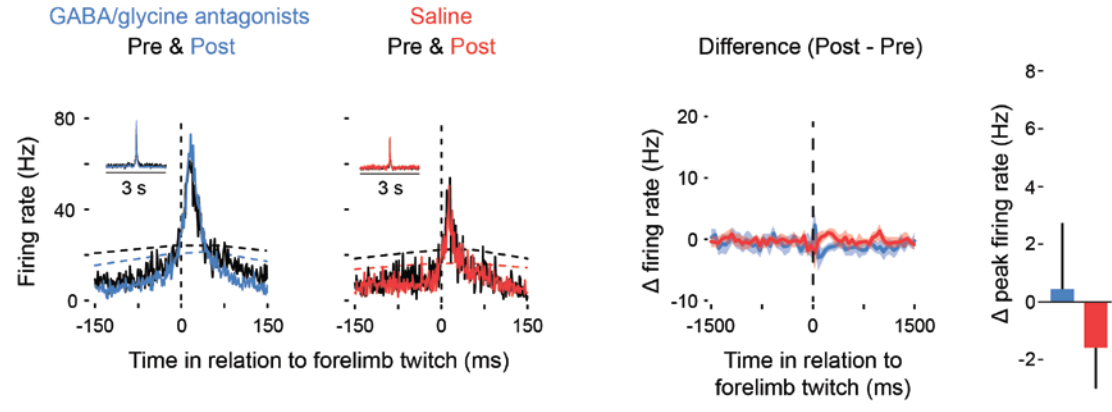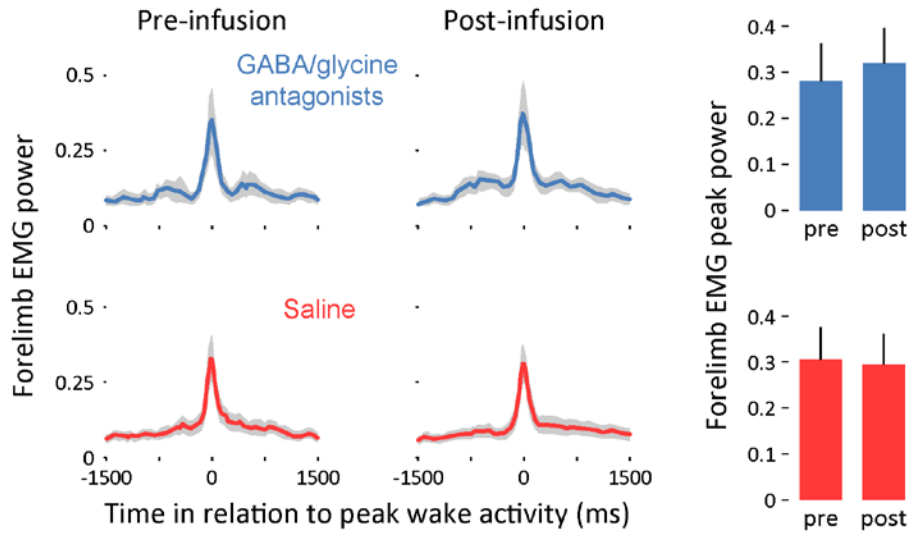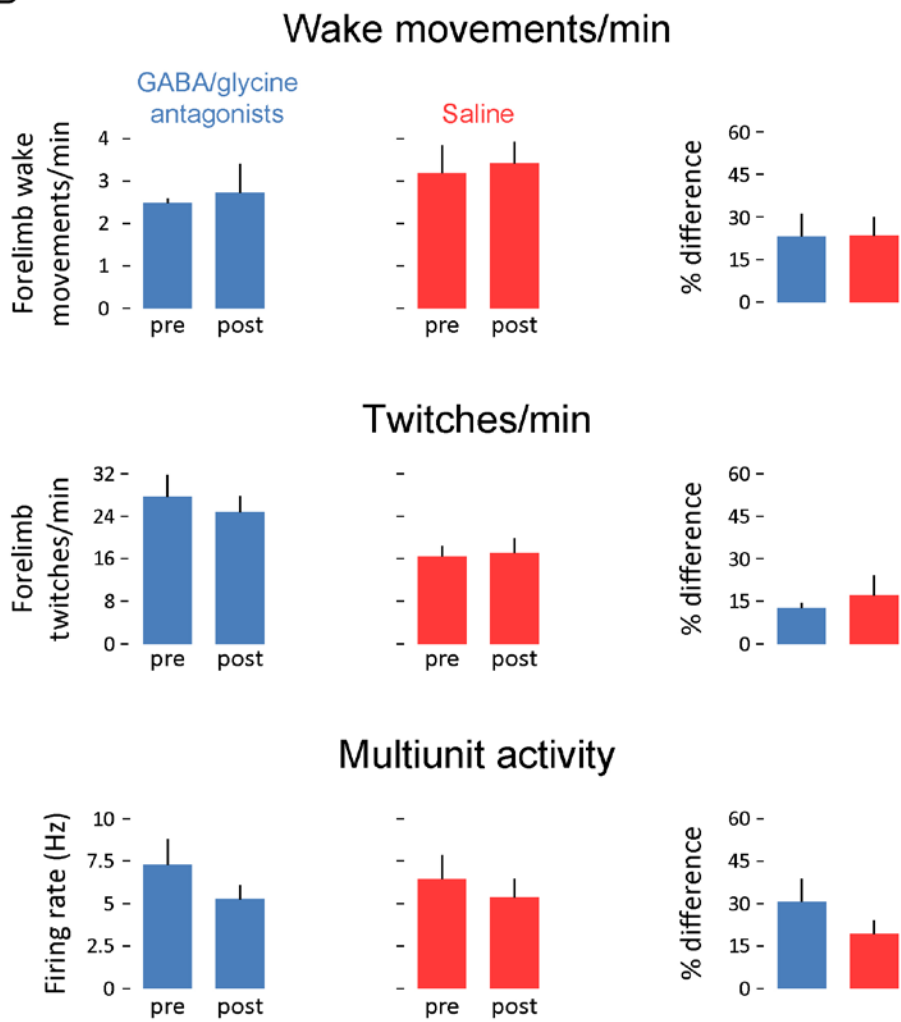
Figure 10. Pharmacological blockade of GABA and glycine receptors in the ECN specifically unmasks reafference from self-generated wake movements. (A) Proposed circuitry depicting how reafference arising from self-

generated movements is modulated at the level of the ECN. Left: During wake, ECN inputs arising from motor areas convey a corollary discharge (i.e., motor copy) signal that gates expected reafference, resulting in decreased activity in the ECN and downstream sensory areas. Right: During active sleep, the motor copy is absent or inhibited and, therefore, ECN inputs arising from motor areas do not gate reafference, resulting in activity in the ECN and downstream sensory areas. (B) ECN recordings were performed using multibarrel electrodes filled with either with a $GABA_A$ antagonist (10 mM bicuculline methiodide) and a glycine antagonist (10 mM strychnine hydrochloride) or saline (n = 5 per group). For all animals, a separate barrel of the electrode was filled with fluorogold (FG) to mark the location of the recording and estimate the spread of the drug (image at bottom right). (C) Left: Event correlations for unit activity in relation to the onset of forelimb wake movements in animals in the GABA/glycine (blue) or saline (red) groups before (Pre) and after (Post) infusion. Data are pooled across all pups. The dashed lines denote upper acceptance bands ($p < 0.05$) for the event correlations. Right: Event correlations depicting the changes in unit activity between the pre-infusion and post-infusion periods for the GABA/glycine (blue) and saline (red) groups. Color-coded shaded regions denote $\pm$SEM. Histograms depict mean (+SEM) peak changes in unit activity (n = 5 per group). * significant difference from saline, $p < 0.05$. (D) Same as in (C) but during active sleep; event correlations are triggered on forelimb twitches.

Figure 11. Pharmacological blockade of GABA and glycine receptors in the ECN does not affect forelimb motor activity or tonic ECN unit activity. (A) Waveform averages (3-s time windows) depicting forelimb EMG power in relation to peak forelimb wake activity before and after infusion of GABA and glycine receptor antagonists (blue) or saline (red). Shaded regions denote $\pm$SEM. At right, mean (+SEM) forelimb EMG peak power derived from waveform averages. (B) Top row: Mean (+SEM) forelimb wake movements/min before and after infusion of GABA and glycine receptor antagonists (blue) or saline (red). At right, mean (+SEM) percent difference (pre vs. post) in forelimb wake movements/min for both experimental groups. Middle and bottom row: Same as top row but for twitches/min and unit activity (in Hz), respectively.
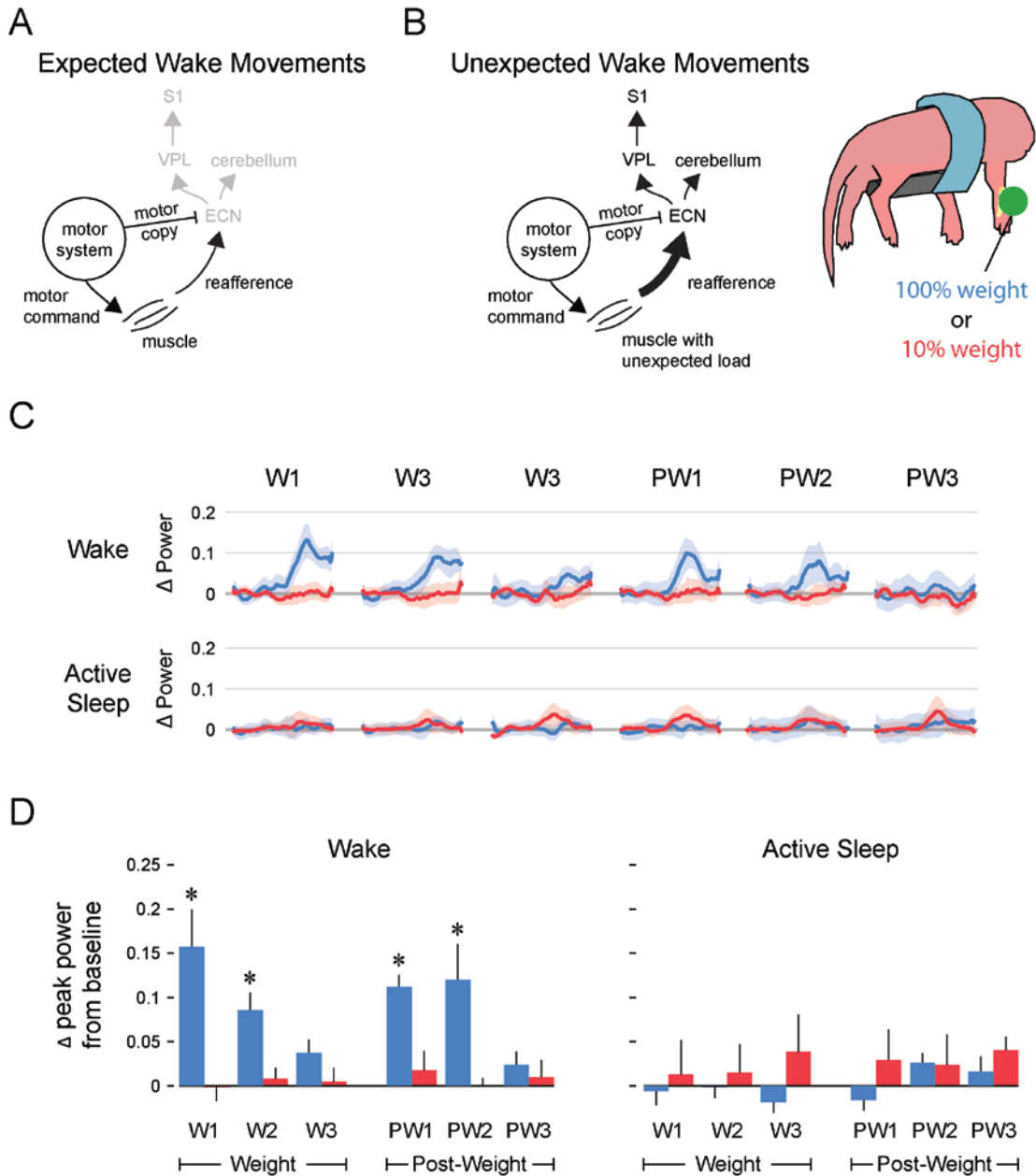
Figure 12. Weighting of the forelimb triggers wake-related reafference in forelimb sensorimotor cortex. (A) Proposed circuitry depicting how reafference is modulated during expected forelimb wake movements. In this case, the corollary discharge (i.e., motor copy) signal matches incoming reafference, resulting in gating of reafference. (B) Attaching a weight to the forelimb produces

an unexpected load, thereby creating a mismatch between the motor copy and reafference signals. The weight was scaled to 10% or 100% of forelimb weight for P8-10 rats. (C) Waveform averages (1-s windows) depicting changes in LFP activity (in relation to the baseline pre-weight period) triggered on the onset of forelimb wake movements or twitches. Data are shown for both limb-weighting conditions (100% or 10% weight, n = 6 pups per group) for the three 15-min time periods with the weight attached (W1-W3) and the three time periods after removal of the weight (PW1-PW3). Color-coded shaded regions denote $\pm$SEM. (D) Mean changes in peak power (+SEM) for the two weighting conditions in relation to peak baseline activity for the weighting and post-weighting time periods. * significant difference from 10% weight group, p < 0.05.
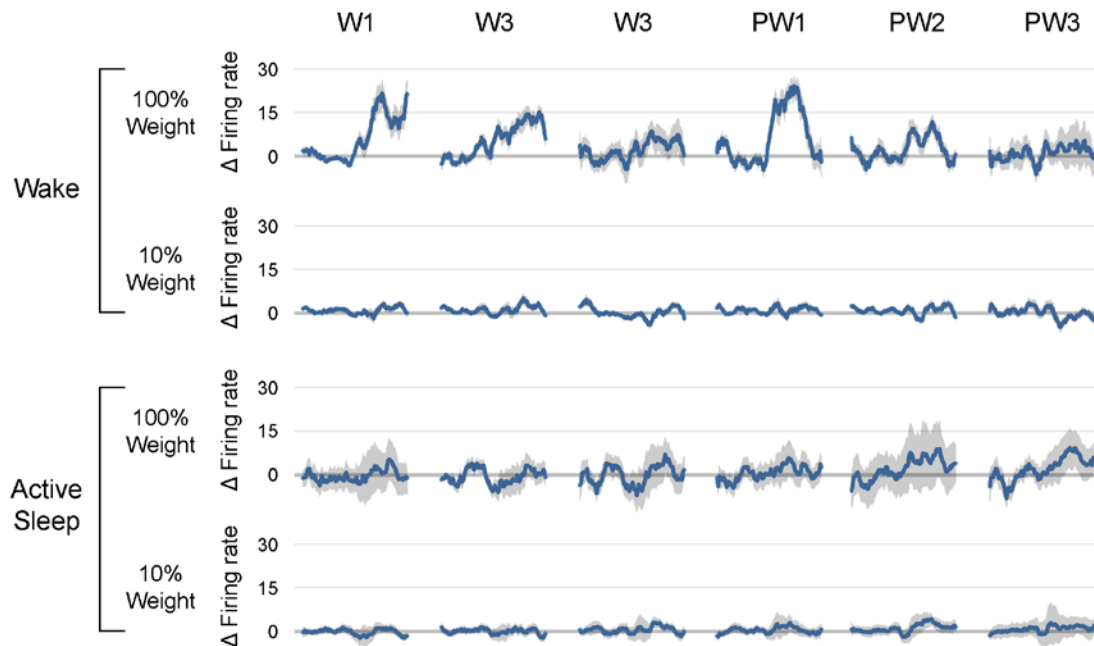
Figure 13. Weighting of the forelimb triggers time-dependent wake-related reafference in forelimb sensorimotor cortex. (A) Event correlations (1-s time windows, 10-ms bins) depicting changes in unit activity (in relation to baseline data) triggered on onset of forelimb twitches or wake movements. Data are shown for both the 100% (n = 20 units) and 10% (n = 17 units) conditions for the three 15-min time periods with the weight attached (W1-W3) and the three time periods after removal of the weight (PW1-PW3). Shaded regions denote ±SEM.

CHAPTER 4: OVERVIEW AND SIGNIFICANCE OF RESEARCH

The collection of studies presented here provide evidence that twitches, but not wake movements, robustly activate the sensory neuraxis, from the brainstem (ECN) to the cerebral cortex (S1 & M1). Therefore, despite both twitches and wake-related movements being self-generated, they are differentially processed by the nervous system. To explain why this difference occurs, we hypothesized that wake-related reafference is suppressed due to the inhibitory actions of corollary discharge during self-generated movements. In contrast, we hypothesized that twitch-related reafference is robust because twitches are not accompanied by the inhibitory actions of corollary discharge.

If corollary discharge mechanisms indeed suppress wake-related reafference, then introducing discrepancies between corollary discharge and expected feedback should result in newfound activity. Indeed, whether we induced wake movements that bypassed much of the corollary discharge circuitry (Chapter 2), manipulated reafference (Chapter 3), or inhibited the corollary discharge circuitry (Chapter 3), all such manipulations resulted in increased neural activity during wake movements. Moreover, consistent with our hypothesis that corollary discharge mechanisms do not accompany twitches, the above manipulations had no effect on twitch-related reafference.

To our knowledge, the ECN has never before been recorded from in unanesthetized animals. Doing so allowed us to determine that proprioceptive feedback is modulated just one synapse away from peripheral receptors.

Interestingly, proprioceptive feedback is likely again modulated in the cerebellum, which receives both proprioceptive feedback from the ECN and motor input from the pontine nucleus (Huang et al., 2013). This suggests that there are likely multiple loops of sensory modulation throughout the neuraxis, perhaps serving different functions at various levels (Del Rio-Bermudez et al., 2015).

In addition, and perhaps most important, the ECN only modulates reafference during wake movements; during sleep, the ECN does not gate twitch-related reafference. Therefore, the data suggest that the ECN is a state-dependent comparator of planned and performed actions. But what functional purpose might a state-dependent comparator serve?

Complex everyday behavior depends on the continuous comparison of planned and performed actions. For example, disruption of corollary discharge pathways has a profound negative impact on forelimb reaching (Azim et al., 2014) and control of eye movements (Sommer and Wurtz, 2002). In this context, the modulation of wake-related reafference within the ECN makes functional sense. But if sensory gating is critical for motor function, why suppress this mechanism during active sleep?

The absence of sensory gating during sleep raises the possibility that corollary discharge mechanisms interfere with functional processes in which twitches are involved. Indeed, if sensory gating were to occur during active sleep, twitches— which are especially abundant during early development—would trigger little or no reafference. In the context of a developing system that requires activity for many activity-dependent processes (Kirkby et al., 2013), the gating of

reafference would suppress the very activity upon which these processes depend. Because reafference is not gated during sleep as it is during wake, twitches are permitted to activate the sensory neuraxis—including the ECN (as shown here), and also the red nucleus (Del Rio-Bermudez et al., 2015), cerebellum (Sokoloff et al., 2015a, 2015b), thalamus (Khazipov et al., 2004; Tiriac et al., 2012), sensorimotor cortex (Khazipov et al., 2004; Tiriac et al., 2014), and hippocampus (Mohns and Blumberg, 2010). The very presence of a state-dependent neural comparator argues both for the importance of sensory gating during wake and the absence of sensory gating during sleep. With regard to the latter, the identification here of a precise neural mechanism that distinguishes twitches from wake movements reinforces the notion that twitches are uniquely able to drive the development and refinement of sensorimotor circuits (Blumberg et al., 2013b).

REFERENCES

Alstermark, B., Isa, T., Pettersson, L.G., Sasaki, S., 2007. The C3-C4 propriospinal system in the cat and monkey: A spinal pre-motoneuronal centre for voluntary motor control. Acta Physiol. 189, 123–140.

Amarasingham, A., Harrison, M.T., Hatsopoulos, N.G., Geman, S., 2011. Conditional modeling and the jitter method of spike re-sampling: Supplement. J Neurophysiol arXiv. Ava.

Amarasingham, A., Harrison, M.T., Hatsopoulos, N.G., Geman, S., 2012. Conditional modeling and the jitter method of spike resampling. J. Neurophysiol. 107, 517–31.

An, S., 2013. Long-term potentiation and neural network activity in the neonatal rat cerebral cortex in vivo.

Andersen, P., Eccles, J.C., Schmidt, R.F., Yokota, T., 1964. Depolarization of presynaptic fibers in the cuneate nucleus. J. Neurophysiol. 27, 92–106.

Azim, E., Jiang, J., Alstermark, B., Jessell, T.M., 2014. Skilled reaching relies on a V2a propriospinal internal copy circuit. Nature 508, 357–363.

Bell, C.C., 1989. Sensory coding and corollary discharge effects in mormyrid electric fish. J. Exp. Biol. 146, 229–53.

Bell, C.C., 2001. Memory-based expectations in electrosensory systems. Curr. Opin. Neurobiol.

Blumberg, M.S., Coleman, C.M., Gerth, A.I., McMurray, B., 2013a. Spatiotemporal structure of REM sleep twitching reveals developmental origins of motor synergies. Curr. Biol. 23, 2100–9.

Blumberg, M.S., Marques, H.G., Iida, F., 2013b. Twitching in sensorimotor development from sleeping rats to robots. Curr. Biol. 23, R532–R537.

Blumberg, M.S., Sokoloff, G., Tiriac, A., Del Rio-Bermudez, C., 2015. A valuable and promising method for recording brain activity in behaving newborn rodents. Dev. Psychobiol. 57, 506–17.

Boivie, J., Boman, K., 1981. Termination of a separate (proprioceptive?) cuneothalamic tract from external cuneate nucleus in monkey. Brain Res. 224, 235–246.

Brooks, J.X., Carriot, J., Cullen, K.E., 2015. Learning to expect the unexpected: rapid updating in primate cerebellum during voluntary self-motion. Nat. Neurosci. 18, 1–10.

Brooks, J.X., Cullen, K.E., 2013. The primate cerebellum selectively encodes unexpected self-motion. Curr. Biol.

Brooks, J.X., Cullen, K.E., 2014. Early vestibular processing does not discriminate active from passive self-motion if there is a discrepancy between predicted and actual proprioceptive feedback. J. Neurophysiol. 111, 2465–78.

Brumley, M.R., Robinson, S.R., 2005. The serotonergic agonists quipazine, CGS-12066A, and alpha-methylserotonin alter motor activity and induce hindlimb stepping in the intact and spinal rat fetus. Behav. Neurosci. 119, 821–33.

Campbell, S.K., Parker, T.D., Welker, W., 1974. Somatotopic organization of the external cuneate nucleus in albino rats. Brain Res. 77, 1–23.

Caputi, A.A., 2004. Contributions of electric fish to the understanding of sensory processing by reafferent systems. J. Physiol. Paris 98, 81–97.

Cooke, J.D., Larson, B., Oscarsson, O., Sjölund, B., 1971. Origin and termination of cuneocerebellar tract. Exp. Brain Res. 13, 339–358.

Crapse, T.B., Sommer, M.A., 2008. Corollary discharge across the animal kingdom. Nat. Rev. Neurosci. 9, 587–600.

Cullen, K.E., 2004. Sensory signals during active versus passive movement. Curr. Opin. Neurobiol.

Del Rio-Bermudez, C., Sokoloff, G., Blumberg, M.S., 2015. Sensorimotor processing in the newborn rat red nucleus during active sleep. J. Neurosci. 35, 8322–32.

Edwards, S.B., 1972. The ascending and descending projections of the red nucleus in the cat: an experimental study using an autoradiographic tracing method. Brain Res. 48, 45–63.

Franklin, D.W., Wolpert, D.M., 2011. Computational mechanisms of sensorimotor control. Neuron 72, 425–42.

Frith, C.D., Blakemore, S., Wolpert, D.M., 2000. Explaining the symptoms of schizophrenia: abnormalities in the awareness of action. Brain Res. Rev. 31, 357–63.

Galindo, A., Krnjević, K., Schwartz, S., 1967. Micro-iontophoretic studies on neurones in the cuneate nucleus. J. Physiol. 192, 359–77.

Gassel, M.M., Marchiafava, P.L., Pompeiano, O., 1964. Phasic changes in muscular activity during desynchronyzed sleep in unrestrained cats. Arch. Ital. Biol. 102, 449–70.

Gramsbergen, A., Schwartze, P., Prechtl, H.F., 1970. The postnatal development of behavioral states in the rat. Dev. Psychobiol. 3, 267–80.

Haggard, P., Whitford, B., 2004. Supplementary motor area provides an efferent signal for sensory suppression. Cogn. Brain Res. 19, 52–58.

Hantman, A.W., Jessell, T.M., 2010. Clarke's column neurons as the focus of a corticospinal corollary circuit. Nat. Neurosci. 13, 1233–9.

Harrison, M.T., Geman, S., 2009. A rate and history-preserving resampling algorithm for neural spike trains. Neural Comput. 21, 1244–58.

Hatsopoulos, N.G., Suminski, A.J., 2011. Sensing with the motor cortex. Neuron 72, 477–87.

Hedwig, B., 2006. Pulses, patterns and paths: Neurobiology of acoustic behaviour in crickets. J. Comp. Physiol. A 192, 677–689.

Heino, R., Westman, J., 1991. Quantitative analysis of the feline dorsal column nuclei and their GABAergic and non-GABAergic neurons. Anat. Embryol. (Berl). 184, 181–193.

Holst, E., Mittelstaedt, H., 1950. The principle of reafference: Interactions between the central nervous system and the peripheral organs. Naturwissenschaften 37, 464–476.

Holstege, G., Tan, J., 1988. Projections from the red nucleus and surrounding areas to the brainstem and spinal cord in the cat. An HRP and autoradiographical tracing study. Behav. Brain Res. 28, 33–57.

Huang, C.C., Sugino, K., Shima, Y., Guo, C., Bai, S., Mensh, B.D., Nelson, S.B., Hantman, A.W., 2013. Convergence of pontine and proprioceptive streams onto multimodal cerebellar granule cells. Elife 2013, 1–17.

Jouvet-Mounier, D., Astic, L., Lacote, D., 1970. Ontogenesis of the states of sleep in rat, cat, and guinea pig during the first postnatal month. Dev. Psychobiol. 2, 216–239.

Karlsson, K.A.E., Gall, A.J., Mohns, E.J., Seelke, A.M.H., Blumberg, M.S., 2005. The neural substrates of infant sleep in rats. PLoS Biol. 3, 0891–0901.

Kennedy, A., Wayne, G., Kaifosh, P., Alviña, K., Abbott, L.F., Sawtell, N.B., 2014. A temporal basis for predicting the sensory consequences of motor commands in an electric fish. Nat. Neurosci. 17, 416–22.

Khazipov, R., Sirota, A., Leinekugel, X., Holmes, G.L., Ben-Ari, Y., Buzsáki, G., 2004. Early motor activity drives spindle bursts in the developing somatosensory cortex. Nature 432, 758–61.

Kirkby, L.A., Sack, G.S., Firl, A., Feller, M.B., 2013. A role for correlated spontaneous activity in the assembly of neural circuits. Neuron 80, 1129–44.

Kreider, J.C., Blumberg, M.S., 2000. Mesopontine contribution to the expression of active "twitch" sleep in decerebrate week-old rats. Brain Res. 872, 149–59.

Kubota, K., Tanaka, R., 1968. Fusimotor unit activities and natural sleep in the cat. Jpn. J. Physiol. 18, 43–58.

Li, D., 2015. Role for the red nucleus in motor control during REM sleep. Masters Thesis.

Mackie, P.D., Morley, J.W., Rowe, M.J., 1999. Signalling of static and dynamic features of muscle spindle input by external cuneate neurones in the cat. J. Physiol. 519 Pt 2, 559–69.

Marcano-Reik, A.J., Prasad, T., Weiner, J.A., Blumberg, M.S., 2010. An abrupt developmental shift in callosal modulation of sleep-related spindle bursts coincides with the emergence of excitatory-inhibitory balance and a reduction of somatosensory cortical plasticity. Behav. Neurosci. 124, 600–11.

Marques, H.G., Imtiaz, F., Iida, F., Pfeifer, R., 2013. Self-organization of reflexive behavior from spontaneous motor activity. Biol. Cybern. 107, 25–37.

Martin, G.F., Dom, R., Katz, S., King, J.S., 1974. The organization of projection neurons in the opossum red nucleus. Brain Res. 78, 17–34.

McVea, D.A., Mohajerani, M.H., Murphy, T.H., 2012. Voltage-sensitive dye imaging reveals dynamic spatiotemporal properties of cortical activity after spontaneous muscle twitches in the newborn rat. J. Neurosci. 32, 10982–94.

Milh, M., Kaminska, A., Huon, C., Lapillonne, A., Ben-Ari, Y., Khazipov, R., 2007. Rapid cortical oscillations and early motor activity in premature human neonate. Cereb. cortex 17, 1582–1594.

Mohns, E.J., Blumberg, M.S., 2008. Synchronous bursts of neuronal activity in the developing hippocampus: modulation by active sleep and association with emerging gamma and theta rhythms. J. Neurosci. 28, 10134–44.

Mohns, E.J., Blumberg, M.S., 2010. Neocortical activation of the hippocampus during sleep in infant rats. J. Neurosci. 30, 3438–3449.

Petersson, P., Waldenström, A., Fåhraeus, C., Schouenborg, J., 2003. Spontaneous muscle twitches during sleep guide spinal self-organization. Nature 424, 72–5.

Pivetta, C., Esposito, M.S., Sigrist, M., Arber, S., 2014. Motor-circuit communication matrix from spinal cord to brainstem neurons revealed by developmental origin. Cell 156, 537–548.

Poulet, J.F.A., Hedwig, B., 2006. The cellular basis of a corollary discharge. Science (80-.). 311, 518–22.

Poulet, J.F.A., Hedwig, B., 2007. New insights into corollary discharges mediated by identified neural pathways. Trends Neurosci. 30, 14–21.

Proske, U., Gandevia, S., 2012. The proprioceptive senses: their roles in signaling body shape, body position and movement, and muscle force. Physiol. Rev.

Robinson, S.R., Blumberg, M.S., Lane, M.S., Kreber, L.A., 2000. Spontaneous motor activity in fetal and infant rats is organized into discrete multilimb bouts. Behav. Neurosci. 114, 328–36.

Robinson, S.R., Kleven, G.A., Brumley, M.R., 2008. Prenatal development of interlimb motor learning in the rat fetus. Infancy 13, 204–228.

Roffwarg, H.P., Muzio, J.N., Dement, W.C., 1966. Ontogenetic development of the human sleep-dream cycle. Science (80-.). 152, 604–619.

Roy, J.E., Cullen, K.E., 2004. Dissociating self-generated from passively applied head motion: neural mechanisms in the vestibular nuclei. J. Neurosci. 24, 2102–11.

Sato, K., Zhang, J.H., Saika, T., Sato, M., Tada, K., Tohyama, M., 1991. Localization of glycine receptor alpha 1 subunit mRNA-containing neurons in the rat brain: an analysis using in situ hybridization histochemistry. Neuroscience 43, 381–95.

Sawtell, N.B., 2010. Multimodal integration in granule cells as a basis for associative plasticity and sensory prediction in a cerebellum-like circuit. Neuron 66, 573–84.

Scriba, M.F., Ducrest, A.-L., Henry, I., Vyssotski, A.L., Rattenborg, N.C., Roulin, A., 2013. Linking melanism to brain development: expression of a melanism-related gene in barn owl feather follicles covaries with sleep ontogeny. Front. Zool. 10, 42.

Seelke, A.M.H., Blumberg, M.S., 2008. The microstructure of active and quiet sleep as cortical delta activity emerges in infant rats. Sleep 31, 691–9.

Seelke, A.M.H., Karlsson, K.A.E., Gall, A.J., Blumberg, M.S., 2005. Extraocular muscle activity, rapid eye movements and the development of active and quiet sleep. Eur. J. Neurosci. 22, 911–20.

Seki, K., Perlmutter, S.I., Fetz, E.E., 2003. Sensory input to primate spinal cord is presynaptically inhibited during voluntary movement. Nat. Neurosci. 6, 1309–1316.

Shipp, S., Adams, R.A., Friston, K.J., 2013. Reflections on agranular architecture: predictive coding in the motor cortex. Trends Neurosci. 36, 706–16.

Sokoloff, G., Plumeau, A.M., Mukherjee, D., Blumberg, M.S., 2015a. Twitch-related and rhythmic activation of the developing cerebellar cortex. J. Neurophysiol. 114, jn.00284.2015.

Sokoloff, G., Uitermarkt, B.D., Blumberg, M.S., 2015b. REM sleep twitches rouse nascent cerebellar circuits: Implications for sensorimotor development. Dev. Neurobiol. 75, 1140–1153.

Sommer, M.A., Wurtz, R.H., 2002. A pathway in primate brain for internal monitering of movements. Science (80-.). 296, 1480–1482.

Sommer, M.A., Wurtz, R.H., 2008. Brain circuits for the internal monitoring of movements. Annu. Rev. Neurosci. 31, 317–38.

Sperry, R., 1950. Neural basis of the spontaneous optokinetic response produced by visual inversion. J. Comp. Physiol. Psychol.

Stefani, A., Gabelia, D., Mitterling, T., Poewe, W., Högl, B., Frauscher, B., 2015. A prospective video-polysomnographic analysis of movements during physiological sleep in 100 healthy sleepers. Sleep 38, 1479–87.

Thurber, A., Jha, S.K., Coleman, T., Frank, M.G., 2008. A preliminary study of sleep ontogenesis in the ferret (Mustela putorius furo). Behav. Brain Res. 189, 41–51.

Tiriac, A., Del Rio-Bermudez, C., Blumberg, M.S., 2014. Self-generated movements with "unexpected" sensory consequences. Curr. Biol. 24, 2136–2141.

Tiriac, A., Uitermarkt, B.D., Fanning, A.S., Sokoloff, G., Blumberg, M.S., 2012. Rapid whisker movements in sleeping newborn rats. Curr. Biol. 22, 2075–2080.

Todd, W.D., Gibson, J.L., Shaw, C.S., Blumberg, M.S., 2010. Brainstem and hypothalamic regulation of sleep pressure and rebound in newborn rats. Behav. Neurosci. 124, 69–78.

Voss, M., Ingram, J.N., Haggard, P., Wolpert, D.M., 2006. Sensorimotor attenuation by central motor command signals in the absence of movement. Nat. Neurosci. 9, 26–27.

Wise, A.K., Gregory, J.E., Proske, U., 1999. The responses of muscle spindles to small, slow movements in passive muscle and during fusimotor activity. Brain Res. 821, 87–94.

Wolpert, D.M., Miall, R.C., Kawato, M., 1998. Internal models in the cerebellum. Trends Cogn. Sci. 2, 338–47.